

# Temporal Query Networks for Fine-grained Video Understanding

Chuhan Zhang  
University of Oxford  
czhang@robots.ox.ac.uk

Ankush Gupta  
DeepMind, London  
ankushgupta@google.com

Andrew Zisserman  
University of Oxford  
az@robots.ox.ac.uk

## Abstract

Our objective in this work is fine-grained classification of actions in untrimmed videos, where the actions may be temporally extended or may span only a few frames of the video. We cast this into a query-response mechanism, where each query addresses a particular question, and has its own response label set.

We make the following four contributions: (i) We propose a new model—a Temporal Query Network—which enables the query-response functionality, and a structural understanding of fine-grained actions. It attends to relevant segments for each query with a temporal attention mechanism, and can be trained using only the labels for each query. (ii) We propose a new way—stochastic feature bank update—to train a network on videos of various lengths with the dense sampling required to respond to fine-grained queries. (iii) We compare the TQN to other architectures and text supervision methods, and analyze their pros and cons. Finally, (iv) we evaluate the method extensively on the FineGym and Diving48 benchmarks for fine-grained action classification and surpass the state-of-the-art using only RGB features.

Webpage: <http://www.robots.ox.ac.uk/~vgg/research/tqn/>.

## 1. Introduction

Imagine that you wish to answer particular questions about a video. These questions could be quite general, *e.g.*, “what instrument is being played?”, quite specific, *e.g.*, “do people shake hands?”, or require a composite answer, *e.g.*, “how many somersaults, if any, are performed in this video, and where?”. Answering these questions will in general require attending to the entire video (to ensure that nothing is missed), and the response is *query dependent*. Further, the response may depend on only a very few frames where a subtle action occurs. With such video understanding capability, it is possible to effortlessly carry out regular video metrology such as performance evaluation in sports training, or issuing reports on video logs.

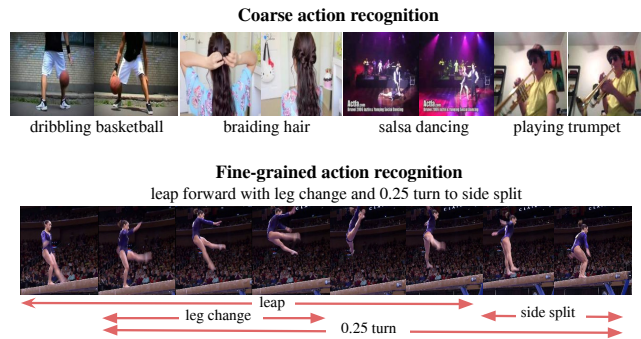


Figure 1: **Coarse vs. fine-grained action recognition.** **Top:** Object and background cues from only a few frames can inform classic coarse-grained action recognition in datasets like Kinetics [30], where visually distinct activities are to be distinguished. **Bottom:** However, for finer-grain classification which depends on subtle differences in pose, the specific sequence, duration and number of certain sub-actions, as for the gymnastics sequence above, requires reasoning about events at varying temporal scales and attention to fine details. We develop a novel query-based video network and a training framework for such fine-grained temporal reasoning.

The objective of this paper is a network and training framework that will enable questions of various granularity to be answered on a video. Specifically, we consider *untrimmed videos* and train with *weak supervision*, meaning that at training time we are not provided with the temporal localization information for the response. To this end, we introduce a new Transformer-based [61] video network architecture, the *Temporal Query Network* (TQN), for fine-grained action classification. The TQN ingests a video and a pre-defined set of *queries* and outputs *responses* for each query, where the response is query dependent.

The queries act as ‘experts’ that are able to pick out from the video the temporal segments required for their response. Since the temporal position of the response is unknown, they must examine the entire duration of the video and be able to ignore irrelevant content, in a similar manner to a

‘matched filter’ [59]. Furthermore, since the duration of response segments may only be a few frames, excessive temporal aggregation (for example, by average pooling the entire untrimmed video) may lose the signal in the noise.

As the TQN must attend *densely* to the video frames for answering specific queries, and cannot sub-sample in time, we also introduce a *stochastically updated feature bank* so that the model can be trained beyond the constraints imposed by finite GPU memory. For this we use a temporal feature bank in which features from densely sampled contiguous temporal segments are cached over the course of training, and only a random subset of these features is computed online and backpropagated through in each training iteration.

We demonstrate the TQN on two fine-grained action recognition datasets with untrimmed video sequences: FineGym [49] and Diving48 [40]. Both of these datasets share the following challenges: (i) object and backgrounds cannot be used to inform classification, as is possible for more coarse-grained action recognition datasets, *e.g.*, Kinetics [30] and UCF-101 [53] (see Figure 1). (ii) subtle differences in actions, relative spatial orientations and temporal ordering of objects/actors need to be distinguished. (iii) events have a short duration of approx. 0.3 seconds in video clips which are typically 6-10 seconds long, and can be as much as 30 seconds in length. (iv) Finally, the duration and position of events vary and is unknown in training. This lack of alignment between text-description (labels) and videos means that that supervision is weak.

**Summary of contributions:** (i) we introduce a new model—a Temporal Query Network (TQN)—which enables query-response functionality on untrimmed videos. It can be trained using only the labels for each query. We show how fine-grained video classification can be cast as a query-response task. (ii) We propose a new way—stochastic feature bank update—to train a network on videos of various lengths with the dense sampling required to respond to fine-grained queries. (iii) We compare the TQN to other architectures and text supervision methods, and analyze their pros and cons. Finally, (iv) we evaluate the method extensively on the FineGym [49] and Diving48 [40] benchmarks for fine-grained action classification. We demonstrate the benefits of the TQN and stochastic feature bank update over baselines and with ablations, and the importance of extended and dense temporal context. The TQN with stochastic feature bank update training surpass the state-of-the-art on these two benchmarks using only RGB features.

## 2. Related Work

**Action Recognition.** Convolutional neural network have been widely used in action recognition recently, including both 2D networks like the two-stream [52],

TSN [64], TRN [80], TSM [43], TPN [75], and 3D networks like LTC [60], I3D [6], S3D [72], SlowFast [15], X3D [14]. Progress in architectures has led to a steadily improved performance on both coarse and fine-grained action datasets [10, 30, 35, 53]. Despite this success, challenges remain: fine-grained action recognition without objects and background biases [9, 40], long-term action understanding [68, 77], and distinguishing actions with subtle differences [49].

**Long-Term Video Understanding.** Early work used RNNs like LSTM [24] for context-modeling in long videos [39, 41]. More recently, the Transformer [61] architecture has been widely adopted for vision tasks due to its advantage in modeling long-term dependencies. The combination of ConvNets and Transformer is applied not only for images [5, 7, 11, 13, 81], but also on video tasks including representation learning [16, 54, 55], and action classification [19, 65, 68].

**Video-Text Representation Learning.** Videos are naturally rich in modalities, and text extracted from associated captions, audio, and transcripts is often used for video representation learning. [4, 25] use text as weak supervision to localize actions through alignment, but require text to have the same order as actions. [1, 22] learn to localize and detect action from sparse text labels, while [17] focuses on localizing actions in untrimmed videos by aligning free-form sentences, whereas we learn to answer specific questions with a pre-defined response set. Text is also used in self-supervised text-video representation learning [46, 48, 55], or for supervised tasks like video retrieval [8, 16, 44, 67].

**Overcoming Memory Constraints in Frame Sampling.** A common way to extract features from a video is by sampling a fixed number of frames, usually less than 64 [6, 43, 72]. However, such coarse sampling of frames is not sufficient, especially for fine-grained actions in untrimmed videos [21, 40, 49, 51]. One common solution is to use pre-trained features [18, 37, 47, 56, 68], but this relies on good initializations and ensuring a small domain gap. While another solution focuses on extracting key frames from untrimmed videos [20, 34].

**Visual Question and Answering (VQA).** Models for VQA usually have queries which attend to relevant features for predicting the answers [32, 38, 42, 79]. For example, [26] use co-attention between vision and language, and [76] adapts attribute-based attention in LSTM using a pertained attribute detector. [31] proposes a progressive attention memory to progressively prune out irrelevant temporal parts. Our query decoder has a similar query-response mechanism, however, our final goal is action recognition not VQA. Instead of having specific questions for each video, we are interested in a common set of queries shared

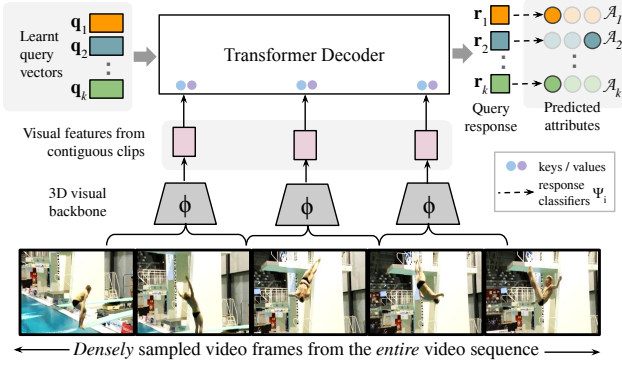


Figure 2: **Temporal Query Network.** A set of permutation-invariant *query vectors*  $\mathbf{q}_i$  are learnt for predefined queries. They attend over densely extracted visual features in a Transformer [61] decoder and generate *response vectors*  $\mathbf{r}_i$ , which are linearly classified ( $\Psi_i$ ) into attributes  $a_i^j$  from corresponding attribute sets  $\mathcal{A}_i$ .

across the whole dataset.

### 3. Method

In this section we first, describe the *Temporal Query Network* (TQN) decoder, which given only weak supervision (no event location/duration), learns to respond to the queries by attending over the entire *densely* sampled untrimmed video (Section 3.1). Second, we introduce a training framework to overcome GPU memory constraints preventing use of temporally-dense video input (Section 3.2). Finally, we explain how the monolithic category labels that are normally provided with fine-grained video datasets, and typically composed of a varying number of sub-labels (or tokens drawn from a finite-set) corresponding to event types and attributes, can be factored into a set of queries and corresponding attributes (Section 3.3).

#### 3.1. Temporal Query Networks

A *Temporal Query Network* (TQN) identifies rapidly occurring discriminative events (spanning only a few frames) in untrimmed videos, and can be trained given only weak supervision, *i.e.*, no temporal location or duration information for events. It achieves this by learning a set of permutation-invariant *query vectors* corresponding to predefined queries about events and their attributes, which are transformed into *response vectors* using Transformer [61] decoder layers attending to visual features extracted from a 3D ConvNet backbone. Figure 2 gives an overview of the model. The visual backbone and the TQN decoder are described below.

**Query-Attributes.** The query set is  $\mathcal{Q} = \{q_i\}_{i=1}^K$ , where each query  $q_i$  has a corresponding attribute set  $\mathcal{A}_i = \{a_1^i, a_2^i, \dots, a_{n_i-1}^i, \emptyset\}$  consisting of the admissi-

ble values  $a_j^i$  in response to  $q_i$ ;  $\emptyset$  denotes the null value (not present), and the total number of attributes  $n_i = |\mathcal{A}_i|$  is query dependent.

For example, in diving videos a query could be the number of turns with the attribute set being the possible counts  $\{0.5, 1.0, 2.5\}$ ; or in gymnastics, the query could be the event type with attributes  $\{\text{vault}, \text{floor-exercise}, \text{balanced beam}\}$ .

**Visual backbone.** Given an untrimmed video, first visual features for contiguous non-overlapping clips of 8 frames are extracted using a 3D ConvNet:  $\Phi = (\Phi_1, \Phi_2, \dots, \Phi_t)$ , where  $t$  is the total number of clips, and  $\Phi_i \in \mathbb{R}^d$  is the  $d$ -dimensional clip-level visual feature. Note, it is important to extract features *densely* from the *entire* length of the video because: (i) it avoids causing temporal aliasing and also missing rapid events (which span only a few frames), *e.g.*, a somersault, and (ii) selecting a subset of clips from the full video for classification [6, 14, 72] is sub-optimal as the location of these events is unknown.

**TQN Decoder.** Given the clip-level features and the label queries, the TQN decoder outputs a *response* for each query. Concretely, for each label query  $q_i$ , a vector  $\mathbf{q}_i \in \mathbb{R}^{d_q}$  is learnt for which a response vector  $\mathbf{r}_i \in \mathbb{R}^{d_q}$  is generated by attending over the visual features  $\Phi$ . Each response vector  $\mathbf{r}_i$  is then linearly classified independently into the corresponding attribute set  $\mathcal{A}_i$ .

In more detail, we use multiple layers of a *parallel non-autoregressive* Transformer decoder, as also used in [5]. Each decoder layer first performs self-attention between the queries, followed by multi-head attention between the updated queries and the visual features. In each attention head, the visual features  $\Phi$  are used to linearly regress *keys*  $\Gamma \cdot \Phi$  and *values*  $\Lambda \cdot \Phi$ , where  $\Gamma$  and  $\Lambda$  are the linear key and value heads. The values are gathered using Softmaxed dot-products between the keys and queries as the weights. Finally, a feed-forward network ingests the values from multiple heads and outputs the response vectors. The response vectors from one decoder layer act as queries for the next layer, except for the first layer where the learnt queries  $\mathbf{q}$  are input. Hence, each decoder layer refines the previously generated response vectors. Mathematically, if  $\ell^{(j)}$  is the  $j$ th decoder layer,  $j \in \{1, 2, \dots, M\}$ :

$$\begin{aligned} \ell^{(j)}(\cdot, \cdot) &: \mathbb{R}^{N \times d_q} \times \mathbb{R}^{t \times d} \mapsto \mathbb{R}^{N \times d_q}, \\ \ell^{(j)}(\mathbf{r}^{(j-1)}, \Phi) &\mapsto \mathbf{r}^{(j)}, \quad \text{and} \\ \mathbf{r}^{(0)} &\triangleq \mathbf{q}. \end{aligned} \tag{1}$$

The response vectors from the final ( $M$ th) layer  $\mathbf{r}_i^{(M)} \in \mathbb{R}^{d_q}$  corresponding to the queries  $\mathbf{q}_i$ ,  $i \in \{1, 2, \dots, K\}$  are classified into the corresponding attribute sets  $\mathcal{A}_i$  using  $K$  independent linear classifiers  $\Psi_i : \mathbb{R}^{d_q} \mapsto \mathbb{R}^{n_i}$ , where  $n_i$  is

the query dependent total number of admissible attributes. Please refer to Figure 2 for a visual representation of this process, and Appendix D for details of the Transformer decoder.

**Training.** The model parameters, *i.e.*, from the visual encoder and the TQN decoder are trained jointly end-to-end with the attribute classifiers  $\Psi_i$  through backpropagation. The training loss is a multi-task combination of individual classifier losses, which are Softmax cross-entropy  $\mathcal{L}_{CE}$  losses on the logits  $\Psi_i \cdot \mathbf{r}_i^{(M)}$  over the attribute sets  $\mathcal{A}_i$ :

$$\mathcal{L}_{\text{total}} = \sum_{i=1}^K \mathcal{L}_{CE}^{(i)}(a^i, \Psi_i \cdot \mathbf{r}_i^{(M)}), \quad (2)$$

where  $a^i$  is the ground-truth attribute for the label query  $q_i$ .

In essence, the TQN decoder learns to establish *temporal correspondence* between the query vectors and the relevant visual features to generate the response. Since the query vectors are themselves learnt, they are optimized to become ‘experts’ which can localize the corresponding event in the untrimmed temporal feature stream. Figures 4 and 5 illustrate this temporal correspondence.

**Discussion: TQN and DETR.** DETR [5] is a recently proposed Transformer based object detection model, which also similarly employs non-autoregressive parallel decoding to output object detections at once. However, there are three crucial differences: (i) the DETR object queries are all equivalent – in that their outputs all specify the same ‘label space’ (object classes and their RoI), essentially queries are *learnt* position encodings. In contrast the TQN queries are distinct from each other and carry a semantic meaning corresponding to event types and attributes; their output response vectors each specify a different set of attributes, and the number of attributes is query dependent. (ii) This leads to the second difference: since the TQN responses are tied to these queries, they can be trained with direct supervision for attribute labels, thereby avoiding train-time Hungarian Matching [36] between prediction and ground-truth employed in DETR. (iii) Finally, no temporal localization supervision is available to the TQN, while (spatial) locations are provided for DETR training. Hence, although TQN is tasked with (implicit) detection of events, it does so with much weaker supervision.

### 3.2. Stochastically Updated Feature Bank

Dense temporal sampling of frames for the entire untrimmed video input is key for detecting rapid discriminative events with unknown temporal location. However, this is challenging in practice due to GPU memory constraints which prevent forwarding densely sampled frames in each training iteration. We use a feature memory bank [70, 71] to overcome these constraints.

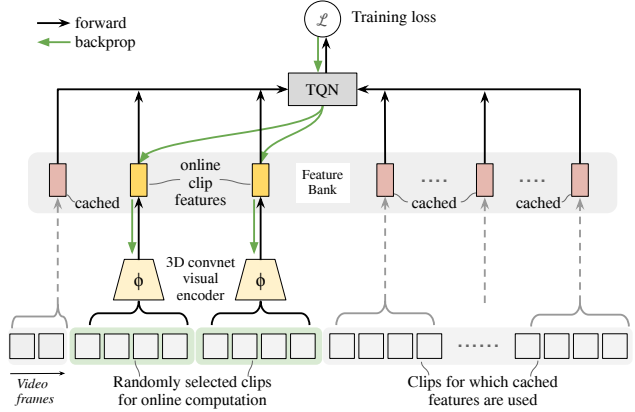


Figure 3: **Stochastically updated feature bank.** Feature banks cache visual encoder features  $\Phi$  to circumvent GPU memory constraints which prevent forwarding densely sampled video frames from the entire length of the video at each training iteration. Randomly sampled contiguous video clips are forwarded online in each iteration and cached immediately; the rest of the clip features are retrieved from the feature bank. The features are then input into the TQN for *joint* training of both the TQN and the visual encoder. This joint training over dense temporal context is critical for fine-grained performance (Section 5.2).

The memory bank caches the clip-level 3D ConvNet visual features. Note for a given video, the clip features  $\Phi = (\Phi_1, \Phi_2, \dots, \Phi_t)$ , where  $t$  is the total number of clips, can be extracted independently of each other. The memory bank is initialized with clip features for all the training videos extracted from a pre-trained 3D ConvNet (details in Section 3.4). Then in each training iteration, a fixed number  $n_{\text{online}}$  of randomly sampled consecutive clips are forwarded through the visual encoder, *i.e.*,  $n_{\text{online}}$  clip features are computed *online*. The remaining  $(t - n_{\text{online}})$  clip features are retrieved from the memory bank. The two sets of visual features are then combined and input into the TQN decoder for final prediction and backpropagation to update the model parameters. Finally, the clip features in the memory bank corresponding to the ones computed online are replaced with the online features. During inference, all the features are computed online without the memory bank. Figure 3 summarizes the function visually.

**Advantages.** Using a fixed number of clips online decouples the length of videos and the GPU memory budget. As a result our memory bank enables the TQN decoder to be trained (i) jointly with the visual encoder, (ii) with extended temporal context, both of which impart drastic improvements in performance (see Section 5.2). Further, it promotes diversity in each mini-batch as multiple different videos can be included instead of just a single long video.

**Discussion: relations with prior memory bank meth-**

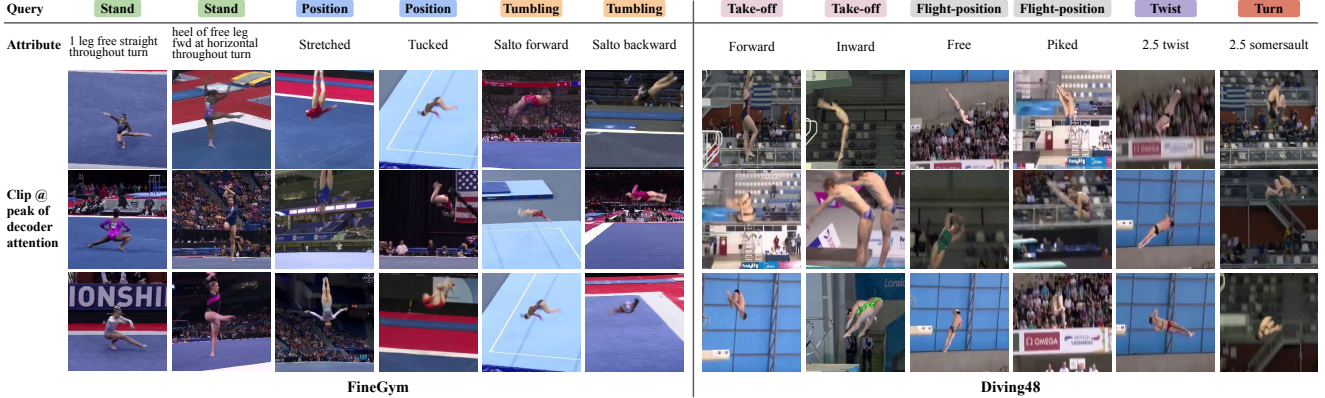


Figure 4: **TQN attention alignment.** For a given query, the TQN attends over the clip-level features to generate the responses. We visualize the central frame from the clip with the highest attention score for six different query-attributes from the FineGym [49] dataset. The same queries (but different attributes) are highlighted with a common color. The TQN detects and aligns semantically relevant events under variations in appearance and pose without any temporal localization supervision. More visualizations in .

**ods.** Feature memory banks have been used for compact vector representations of single images [57, 70, 71], whereas we store a varying number of temporal vectors for each video. MoCo [23] and related self-supervised methods [63, 74] update the memory bank features *slowly* *e.g.*, using a secondary network, to prevent representation collapse, whereas given direct supervision for the queries, we can update the features immediately from the single on-line network. The above works apply memory banks for image/feature retrieval from a large corpus for hard negatives in contrastive training, while we use the memory bank for extending the temporal context for each video. Using pre-computed features [37, 47, 56] or *Long-term Feature Banks* [68] are prominent [2, 18, 69] strategies for extending the temporal support of video models. However, all of these works keep the features *frozen*, while we *continuously update* the memory-bank during training. In Section 5.2, we demonstrate these updates are critical for performance.

### 3.3. Factorizing Categories into Attribute Queries

In this section we illustrate how the pre-defined set of  $N$  categories  $\mathcal{C} = \{c_1, c_2, \dots, c_N\}$  typically associated with

Category ↓	query →	$q_1$ : leap and jump type		$q_2$ : num turns		
	attribute →	switch leap	split jump	0.5	1.0	∅
switch leap w/ 0.5 turn		✓		✓		
switch leap w/ 1 turn		✓			✓	
split jump w/ 1 turn			✓		✓	
split jump			✓			✓

Table 1: **Illustration of query-attribute factorization of fine-grained action categories.** Four categories are factored into two queries  $q_1, q_2$  with two and three attributes respectively.

fine-grained video recognition datasets can be factored into attribute queries. In such datasets, the categories differ in subtle details *e.g.*, the specific type, duration, or count of a certain sequence of events. These can be rapidly occurring (short duration) events with unknown temporal location and duration (see Figure 1).

The textual descriptions of categories  $\mathcal{C}$  are strings composed of a varying number of sub-labels (or tokens drawn from a finite-set) corresponding to event types and attributes (sub-label categories). We leverage this string structure to form queries  $\{q_i\}_{i=1}^K$  corresponding to sub-label categories, each with an associated attribute set  $\mathcal{A}_i$  composed of sub-labels, such that the categories  $\mathcal{C}$  can be expressed as a subset of the cartesian product of the attribute sets:  $\mathcal{C} \subseteq \mathcal{A}_1 \times \mathcal{A}_2 \times \dots \times \mathcal{A}_K$ . An example label factorization for four categories is given in Table 1, where four action categories are expressed as a product of two attribute sets containing two and three attributes respectively. Factorization details for the evaluation datasets used in this paper are given in Section 4 and Appendix J.

This factorization unpacks the monolithic category labels into their semantic constituents (the queries and attributes). It improves data-efficiency, through sharing video data across common sub-labels (instead of disjoint category-specific data), and induces TQN-style query-based temporal localization and classification video parsing models.

### 3.4. Implementation Details

We describe key model and training details below, with further details in Appendix D.

**Model architecture.** We use S3D [72] as visual backbone, operating on non-overlapping contiguous video clips

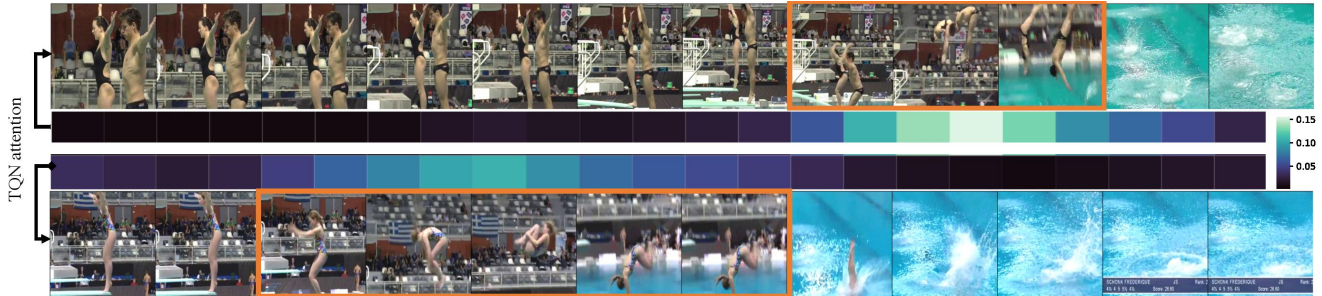


Figure 5: **TQN temporal attention.** Blue colored maps visualize the attention averaged over all queries predicted by TQN for two clips from the Diving48 dataset [40]. The peaks in these maps correspond to temporal location of diving ‘flight’ highlighted in orange. TQN rejects non-informative frames at the start and end of untrimmed videos to localize discriminative frames relevant for fine-grained recognition.

of 8 frames each of size  $224 \times 224$  pixels with consistent temporal stride  $s$  ( $s=1$  in FineGym,  $s=2$  in Diving48), to output one feature vector per clip. The decoder consists of four standard post-normalization [73] Transformer decoder layers [61], each with four attention heads, and 1024-dim keys, (learnt-) queries, and values. Dropout rate is 0.1 in the decoder and 0.5 for output features.

**Training.** The visual encoder is pre-trained on Kinetics-400 [30]. Then, we proceed by a two stage curriculum. First, the model is trained *end-to-end* on *short* videos containing fewer than  $K$  frames (FineGym:  $K = 48$ , Diving48:  $K = 128$ ; as the latter contains approx.  $3 \times$  longer videos), such that they can fit on two Nvidia RTX 6000 GPUs with batch size 16. Second, the model is trained on the whole training set using the stochastically updated memory bank (Section 3.2) to accommodate long videos. We use the Adam optimizer [33], and train for 50 epochs in the first stage, followed by 30 more epochs in the second.

#### 4. Datasets, Baselines, Label Sets, and Metrics

We evaluate TQN for fine-grained action recognition on two video datasets, namely, FineGym [49], and Diving48 [40]. We introduce the datasets, list the baselines methods we compare against, detail the query-attribute based label sets for them, and state the evaluation measure below.

**FineGym.** FineGym is a recently introduced dataset (2020) for fine-grained action understanding, consisting of HD gymnasium classes with subtle motion details. We evaluate for classification under two settings specified in the dataset with standard train/eval splits: (1) Gym99: relatively balanced data for 99 categories with 26k training/8.5k testing videos; and (2) Gym288: long-tailed data for 288 categories with 29k training/9.6k testing videos. There is a large variation in video lengths: min: 13 frames, max: 877 frames, average: 47 frames.

**Diving48.** Diving48 contains competitive diving video

clips from 48 classes. It similarly evaluates fine-grained video recognition by having a common diving setting where subtle details of diving sequences define the various categories instead of coarse objects or scenes. We use the standard split containing 16k training/2k test videos. The video lengths have a very wide range: min: 24 frames, max: 822 frames, average: 158 frames. We use the *cleaned-up* labels (denoted ‘v2’) released in Oct 2020. Results for the noisy version (Diving48-v1) can be found in Appendix H.

**Diving48-v2 SotA comparison.** We trained publicly available SotA action recognition models on v2 labels, namely: (i) TSM [43], (ii) TSN [64], (iii) TRNms [80], (iv) I3D [6], (v) S3D [72], and (vi) GST-50 [45]. Note, GST-50 is the top-performing method on Diving48-v1 amongst those using a ResNet-50 backbone (refer to v1 comparison in Appendix H). The original dataset paper [40] reports results only for TSN and C3D [27]; C3D (2013) is omitted as it is outperformed by more recent methods, *e.g.*, I3D and S3D. We could not benchmark against other prominent methods reported for v1, namely, CorrNet [62] and AttnLSTM [28], as their implementation is not public.

**Baseline methods.** Since we use S3D [72] as the visual backbone for TQN, the following two methods form the baselines: (i) **Short-term S3D (ST-S3D):** following the original dataset papers [40, 49], it is trained on single clips of fixed number ( $=8$  if not specified otherwise) of frames, while for inference, the predicted probabilities from multiple clips spanning a given video are averaged for final classification. (ii) **Long-term S3D (LT-S3D = S3D + Feature Bank):** uses our stochastically updated feature bank at training time in order to pool information from the entire video. Specifically, LT-S3D replicates the ST-S3D’s multi-clip evaluation setting at training time, *i.e.*, class probabilities obtained from multiple clips spanning the entire video are averaged and used for prediction and backpropagation.

Note at training time ST-S3D incorrectly bases its decisions on *individual clips* which may not contain information rel-

Backbone	Encoder	Decoder (Aggregation)	Classification	Label	Accuracy	
					per-class	per-video
S3D	-	average pooling	multi-class (cross entropy)	class index	72.3	80.4
		-	-		73.7	80.0
	self-attention	-	multi-label (binary cross entropy)	text descriptions	47.9	50.3
		auto-regressive Transformer	sequence prediction (cross entropy)		51.9	65.1
	-	TQN	multi-task (cross entropy)	-	<b>74.5</b>	<b>81.8</b>

Table 2: **Leveraging multi-part text descriptions.** We compare our *query-attribute* label factorization (Section 3.3) to alternative methods for learning with unaligned (no temporal location information) multi-part text descriptions. Our TQN + label factorization outperforms other approaches which are representative of standard classification, and modern encoder-decoder architectures for sequences (see Section 5.1). Evaluation on the Diving48-v2 dataset.

evant for classification. LT-S3D overcomes this issue using multi-clip feature bank and learns better clip-level features (Section 5.2).

**Label sets: query-attributes.** We define query-attributes independently for each dataset. **Diving48:** The original 48 classes are defined in terms of four *stages* of a diving action. We use four queries corresponding to the stages, and the possible instantiation of each stage as attributes. **FineGym:** Each category in Gym99 and Gym288 is defined by a textual description for the specific sequence *elements* in a gymnastic set, e.g., “*double salto backward tucked with 2 twist*”. We extract nouns from these and categorize them into 12 queries, e.g., *swing, landing, jump and leap, etc.* and their instantiations form the attributes. Complete factorization is specified in Appendix J. In addition to these query and attribute sets, we augment the TQN query set with a “global” query class with the original fine-grained categories as its attribute set, and use its response for the final category prediction.

**Metrics.** We evaluate on (top-1) classification accuracy, both per original class (48 in Diving48, 99 in Gym99 and 288 in Gym288), and per video.

## 5. Experiments

### 5.1. Leveraging Multi-Attribute Labels

We evaluate alternative methods and losses for exploiting multi-part text descriptions on the Diving48-v2 dataset, and compare performance to our *query-attribute* label factorization (Section 3.3). Table 13 summarizes the results for various encoders, decoders and losses; detailed description are given in Appendix G. TQN multi-task losses perform the best (81.8% per-video accuracy), followed by standard multi-class classification (avg. pool: 80.4%, self-attention: 80.0%) which only uses the class index, not the text de-

scriptions. Other sequence based methods for text perform substantially worse (−15-30%), due to the restrictive ordering imposed by the text string. TQN goes beyond just attention-based context aggregation, as it outperforms S3D+attention-encoder trained without queries (2nd row) (81.8% vs. 80.4%). This is most likely due to: (i) data re-use enabled by shared sub-labels; and (ii) the learnt queries act as ‘experts’ to identify discriminative events.

### 5.2. Feature Bank Ablations

We benchmark our stochastically updated feature banks (Section 3.2) in two ways: first, we evaluate the effect of increasing the temporal context during training, and second the effect of backpropagation through the feature bank. We use Diving48-v2 for both.

**Effect of increasing training temporal context.** To evaluate the importance of dense and long temporal context during training for fine-grained action recognition, we train the S3D visual encoder [72] on an increasing number of input frames  $N = \{8, 32, 64, \text{all frames}\}$ , where ‘all frames’ corresponds to LT-S3D, i.e. training with our feature bank. At inference, full temporal support is used for all methods by averaging class probabilities from multiple clips spanning the entire video (no decoder). To control for visual discontinuity between frames due to large input stride, we sample the frames in two ways: (i) *consecutively* sample  $N$  frames with a temporal stride of 2 starting at random temporal locations, and (ii) *uniformly* sample  $N$  frames with a span of the entire video, where the temporal stride  $s$  is proportional to the actual length  $T$  of the video, i.e.,  $s = \lfloor \frac{T}{N} \rfloor$ . Table 5 summarizes the results. Consecutive sampling performs better as uniform sampling implies varying input stride which is not amenable to S3D’s temporal convolutional filters with fixed stride. More importantly, longer temporal context is better regardless of the frame sampling strategy: all frames: 80.5% per-video accuracy; for  $N = \{8, 32, 64\}$ : <75%. This demonstrates the critical role of our feature bank for training.

**Effect of updating bank features during training.** A key difference between our feature bank and previous methods for extended temporal support for videos, e.g., *Long-term feature banks* [68] and [37, 47, 56], is that they use *frozen* features, while we continuously update them. We train with frozen/updated features, with/without the TQN decoder on top of visual features, and summarize the results in Table 4. For both with/without TQN, updating the features improves the performance substantially ( $\approx +15\%$ ). Ablation study of the effect of number of features update on final performance can be found in Appendix E.

Network	Pretrained dataset	Modality	# frames in training	Gym99				Gym288		Diving48-v2	
				Per-class	Per-video			per-class	per-video	per-class	per-video
					subset VT	subset FX	total				
I3D	K400	RGB	8	64.4	47.8	60.2	75.6	28.2	66.7	33.2	48.3
TSN	ImageNet	two-stream	3	79.8	47.5	84.6	86	37.6	79.9	34.8	52.5
TSM	ImageNet	two-stream	3	81.2	44.8	84.9	88.4	46.5	83.1	32.7	51.1
TRNms	ImageNet	two-stream	3	80.2	47.3	84.9	87.8	43.3	82.0	54.4	66.0
GST-50	ImageNet	RGB	8	84.6	53.6	84.9	89.5	46.9	83.8	69.5	78.9
ST-S3D	K400	RGB	8	72.9	45.3	82.8	81.5	42.4	75.8	36.3	50.6
LT-S3D	K400	RGB	dense	88.9	69.1	90.4	92.5	57.9	86.3	72.3	80.4
TQN	K400	RGB	dense	<b>90.6</b>	<b>74.9</b>	<b>91.6</b>	<b>93.8</b>	<b>61.9</b>	<b>89.6</b>	<b>74.5</b>	<b>81.8</b>

Table 3: **Comparison to state-of-the-art.** We compare TQN to several SotA methods for Gym99, Gym288, and Diving48-v2. The results for the Gym datasets are reproduced from the original dataset publication [49], except for S3D [72] and GST-50 [45] was trained by us; no further results are available as the dataset was recently published (2020). For Diving48-v2, since the corrected labels were released recently, we train the publicly available implementations of all methods while replicating the setting of their application to the original Diving48-v1 dataset. TQN achieves top-performance on all three datasets, detailed discussion in Section 5.3.

Description	Visual Encoder	Memory bank	Decoder	Accuracy	
				per-class	per-video
train linear classifier on frozen encoder	frozen	computed offline	avg pool	57.1	66.6
train TQN on frozen encoder			TQN	60.9	68.2
train linear classifier + encoder	fine-tuned	updated online	avg pool	72.3	80.4
train TQN + encoder			TQN	74.5	81.1

Table 4: **Frozen vs. updated feature bank.** To study the importance of updating the feature-bank during training, we train with the TQN decoder and without it (average pooling for temporal aggregation), on top of *frozen* or *stochastically updated* visual features in the memory bank. For both the decoder settings, updating features improves performance drastically ( $\approx +15\%$ ). Evaluation on the Diving48-v2 dataset; details in Section 5.2.

### 5.3. Comparison with State-of-the-art

Finally, in Table 3 we compare the performance of TQN against SotA methods on Diving48-v2, Gym99 and Gym288. For completeness, performance on the original noisy Diving48-v1 is reported in Appendix H. TQN outperforms all methods on all the three benchmarks on both per-video and per-class measures, even when flow+RGB (two-stream) input is allowed for other methods, while only RGB is input to TQN; a detailed table with breakdown for RGB and flow is included in Appendix B. Compared to the ST-S3D baseline (S3D with short temporal context), having long-term context (LT-S3D) using our feature bank leads to drastic improvements:  $>30\%$  (absolute) on Diving48-v2, and  $>10\%$  (absolute) on the Gym datasets. Adding TQN decoder on top of LT-S3D leads to further improvements, notably on the ‘VT’ (vaulting) subset of Gym99 (+5.8%) which contains longer videos: 7–8 seconds compared to 1–2 seconds in the ‘FX’ (floor exercise) subset (+1.2%). Note, the visual backbone of TQN can be made stronger by replacing S3D with, e.g., TSM, TSN, or GST-50. However, we adopt S3D in our experiments as it achieves top performance while fitting within our limited compute budget.

Training				Test (w/ all frames)
temporal support	# frames ( $N$ )	frame sampling	stride	per-video acc
fixed number of frames	8	consecutive	2	58.8
		uniform	–	50.6
	32	consecutive	2	72.9
		uniform	–	71.2
	64	consecutive	2	74.2
		uniform	–	70.0
full temporal support	proportional to length of videos	memory bank	2	<b>80.4</b>

Table 5: **Impact of temporal support during training.** To analyze the importance of temporal support for training and use of stochastically updated feature bank, we train S3D with an increasing number of input frames  $N$  and find that longer temporal context consistently improves performance on Diving48.

### 5.4. Performance on Videos of Different Length

In Figure 6 we plot classification accuracy of TQN and the baseline long-term S3D as a function of video length. On videos shorter than 5 seconds, LT-S3D performs similar to TQN as max-pooling suffices to pick out relevant information in short videos. However, TQN’s attention based classification outperforms simple pooling for longer videos.

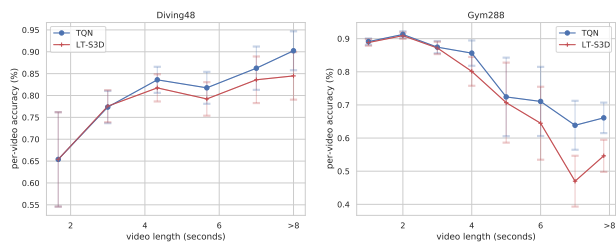


Figure 6: **Classification accuracy on videos of different length.** Mean values plotted with 95% confidence interval.



Pre-training	Epochs	Diving48-v2 top-1
None (random init.)	80	81.8
Gym288	25	83.3

Table 6: **Transferring TQN.** Per-video performance on Diving48-v2 for a TQN model pre-trained on Gym288.

### 5.5. Transfer learning with TQN

To investigate the transferability of TQN across domains which differ visually as well as in their query-attributes, we fine-tune the model pre-trained on Gym288 for Diving48. The query vectors  $\mathbf{q}$  and the response classifiers  $\Psi$  are tied to dataset specific query-attributes. Hence, to fine-tune on a new dataset, we initialize these randomly and retain the initialization from pre-training for other TQN and visual backbone parameters. We compare this to the random initialization baseline in Table 6. We note that fine-tuning gives better accuracy and trains substantially faster as compared to training from scratch. This is likely because the transformer has learnt (and retained) how to match query vectors to temporal events, and encode the event representation for response classifiers. It is thus able to benefit from the additional training data despite the domain shift.

### 5.6. Extension to Multi-label Action Recognition

We apply TQN to the Charades dataset [51] and achieve comparable results with the SotA models. Charades labels multiple actions in one video as different classes with precise temporal annotations, as opposed to classification in FineGym and Diving48 where a sequence of combined actions are labelled as one class without localization. Please refer to Appendix C.

## 6. Conclusion

We have developed a new video parsing model, the Temporal Query Network (TQN), which learns to answer fine-grained questions about event types and their attributes in untrimmed videos. TQN furthers state-of-the-art in fine-grained video categorization on three datasets, and in addition provides temporal localization and alignment of semantically consistent events. The *query-response* mechanism employed in TQN enables efficient data use through sharing training videos across common sub-labels and outperforms alternative strategies for exploiting textual descriptions. The mechanism is more generally applicable to problems which require spotting entities with varying spans in dense data streams. Our training method with stochastically updated feature banks enables such applications without imposing heavy requirements for expensive large-scale training infrastructure.

**Acknowledgements.** This research is funded by a Google-DeepMind Graduate Scholarship, a Royal Society Research Professorship, and the EPSRC Programme Grants Seebibyte EP/M013774/1 and VisualAI EP/T028572/1. We thank Weidi Xie,

Tengda Han and the reviewers for helpful insights.

## References

- [1] Anurag Arnab, Chen Sun, Arsha Nagrani, and Cordelia Schmid. Uncertainty-aware weakly supervised action detection from untrimmed videos. In *Proc. ECCV*, 2020. 2
- [2] Sara Beery, Guanhang Wu, Vivek Rathod, Ronny Votel, and Jonathan Huang. Context r-cnn: Long term temporal context for per-camera object detection. In *Proc. CVPR*, 2020. 5
- [3] Gedas Bertasius, Christoph Feichtenhofer, Du Tran, Jianbo Shi, and Lorenzo Torresani. Learning discriminative motion features through detection. *arXiv preprint arXiv:1812.04172*, 2018. 18
- [4] Piotr Bojanowski, Rémi Lajugie, Edouard Grave, Francis Bach, Ivan Laptev, Jean Ponce, and Cordelia Schmid. Weakly-supervised alignment of video with text. In *Proc. ICCV*, 2015. 2
- [5] Nicolas Carion, Francisco Massa, Gabriel Synnaeve, Nicolas Usunier, Alexander Kirillov, and Sergey Zagoruyko. End-to-end object detection with transformers. In *Proc. ECCV*, 2020. 2, 3, 4
- [6] Joao Carreira and Andrew Zisserman. Quo vadis, action recognition? a new model and the kinetics dataset. In *Proc. CVPR*, 2017. 2, 3, 6, 14, 15, 17
- [7] Mark Chen, Alec Radford, Rewon Child, Jeff Wu, Heewoo Jun, Prafulla Dhariwal, David Luan, and Ilya Sutskever. Generative pretraining from pixels. In *Proc. ICML*, 2020. 2
- [8] Shizhe Chen, Yida Zhao, Qin Jin, and Qi Wu. Fine-grained video-text retrieval with hierarchical graph reasoning. In *Proc. CVPR*, 2020. 2
- [9] Jinwoo Choi, Chen Gao, Joseph CE Messou, and Jia-Bin Huang. Why can't i dance in the mall? learning to mitigate scene bias in action recognition. In *Proc. NeurIPS*, 2019. 2
- [10] Dima Damen, Hazel Doughty, Giovanni Maria Farinella, Sanja Fidler, Antonino Furnari, Evangelos Kazakos, Davide Moltisanti, Jonathan Munro, Toby Perrett, Will Price, et al. Scaling egocentric vision: The epic-kitchens dataset. In *Proc. ECCV*, 2018. 2
- [11] Karan Desai and Justin Johnson. Virtex: Learning visual representations from textual annotations. *arXiv preprint arXiv:2006.06666*, 2020. 2, 17
- [12] Jacob Devlin, Ming-Wei Chang, Kenton Lee, and Kristina Toutanova. Bert: Pre-training of deep bidirectional transformers for language understanding. *arXiv preprint arXiv:1810.04805*, 2018. 17
- [13] Alexey Dosovitskiy, Lucas Beyer, Alexander Kolesnikov, Dirk Weissenborn, Xiaohua Zhai, Thomas Unterthiner, Mostafa Dehghani, Matthias Minderer, Georg Heigold, Sylvain Gelly, et al. An image is worth 16x16 words: Transformers for image recognition at scale. *arXiv preprint arXiv:2010.11929*, 2020. 2, 17
- [14] Christoph Feichtenhofer. X3d: Expanding architectures for efficient video recognition. In *Proc. CVPR*, 2020. 2, 3, 17
- [15] Christoph Feichtenhofer, Haoqi Fan, Jitendra Malik, and Kaiming He. Slowfast networks for video recognition. In *Proceedings of the IEEE international conference on computer vision*, pages 6202–6211, 2019. 2, 15
- [16] Valentin Gabeur, Chen Sun, Karteek Alahari, and Cordelia

- Schmid. Multi-modal Transformer for Video Retrieval. In *Proc. ECCV*, 2020. 2
- [17] Jiyang Gao, Chen Sun, Zhenheng Yang, and Ram Nevatia. Tall: Temporal activity localization via language query. In *Proc. ICCV*, 2017. 2
- [18] Noa Garcia and Yuta Nakashima. Knowledge-based video question answering with unsupervised scene descriptions. In *Proc. ECCV*, 2020. 2, 5
- [19] Rohit Girdhar, Joao Carreira, Carl Doersch, and Andrew Zisserman. Video action transformer network. In *Proc. CVPR*, 2019. 2
- [20] Boqing Gong, Wei-Lun Chao, Kristen Grauman, and Fei Sha. Diverse sequential subset selection for supervised video summarization. In *Proc. NeurIPS*, 2014. 2
- [21] Chunhui Gu, Chen Sun, David A Ross, Carl Vondrick, Caroline Pantofaru, Yeqing Li, Sudheendra Vijayanarasimhan, George Toderici, Susanna Ricco, Rahul Sukthankar, et al. Ava: A video dataset of spatio-temporally localized atomic visual actions. In *Proc. CVPR*, 2018. 2
- [22] Meera Hahn, Nataniel Ruiz, Jean Alayrac, Ivan Laptev, and James M Rehg. Learning to localize and align fine-grained actions to sparse instructions. *arXiv preprint arXiv:1809.08381*, 2018. 2
- [23] Kaiming He, Haoqi Fan, Yuxin Wu, Saining Xie, and Ross Girshick. Momentum contrast for unsupervised visual representation learning. In *Proc. CVPR*, 2020. 5
- [24] Sepp Hochreiter and Jürgen Schmidhuber. Long short-term memory. *Neural computation*, 9(8):1735–1780, 1997. 2
- [25] De-An Huang, Li Fei-Fei, and Juan Carlos Nieves. Connectionist temporal modeling for weakly supervised action labeling. In *Proc. ECCV*, 2016. 2
- [26] Yunseok Jang, Yale Song, Youngjae Yu, Youngjin Kim, and Gunhee Kim. Tgif-qa: Toward spatio-temporal reasoning in visual question answering. In *Proc. CVPR*, 2017. 2
- [27] Shuiwang Ji, Wei Xu, Ming Yang, and Kai Yu. 3d convolutional neural networks for human action recognition. *PAMI*, 2012. 6
- [28] Gagan Kanojia, Sudhakar Kumawat, and Shanmuganathan Raman. Attentive spatio-temporal representation learning for diving classification. In *Proc. CVPR Workshops*, 2019. 6, 18
- [29] Andrej Karpathy, George Toderici, Sanketh Shetty, Thomas Leung, Rahul Sukthankar, and Li Fei-Fei. Large-scale video classification with convolutional neural networks. In *Proc. CVPR*, 2014. 18
- [30] Will Kay, Joao Carreira, Karen Simonyan, Brian Zhang, Chloe Hillier, Sudheendra Vijayanarasimhan, Fabio Viola, Tim Green, Trevor Back, Paul Natsev, Mustafa Suleyman, and Andrew Zisserman. The kinetics human action video dataset. *arXiv preprint arXiv:1705.06950*, 2017. 1, 2, 6, 16, 18
- [31] Junyeong Kim, Minuk Ma, Kyungsu Kim, Sungjin Kim, and Chang D Yoo. Progressive attention memory network for movie story question answering. In *Proc. CVPR*, 2019. 2
- [32] Kyung-Min Kim, Seong-Ho Choi, Jin-Hwa Kim, and Byoung-Tak Zhang. Multimodal dual attention memory for video story question answering. In *Proc. ECCV*, 2018. 2
- [33] D. P. Kingma and J. Ba. Adam: A method for stochastic optimization. In *Proc. ICLR*, 2015. 6
- [34] Bruno Korbar, Du Tran, and Lorenzo Torresani. Scsampler: Sampling salient clips from video for efficient action recognition. In *Proc. ICCV*, 2019. 2
- [35] Hilde Kuehne, Ali Arslan, and Thomas Serre. The language of actions: Recovering the syntax and semantics of goal-directed human activities. In *Proc. CVPR*, 2014. 2
- [36] Harold W Kuhn. The hungarian method for the assignment problem. *Naval research logistics quarterly*, 2(1-2), 1955. 4
- [37] Fu Li, Chuang Gan, Xiao Liu, Yunlong Bian, Xiang Long, Yandong Li, Zhichao Li, Jie Zhou, and Shilei Wen. Temporal modeling approaches for large-scale youtube-8m video understanding. *arXiv preprint arXiv:1707.04555*, 2017. 2, 5, 7
- [38] Xiangpeng Li, Lianli Gao, Xuanhan Wang, Wu Liu, Xing Xu, Heng Tao Shen, and Jingkuan Song. Learnable aggregating net with diversity learning for video question answering. In *Proceedings of the 27th ACM International Conference on Multimedia*, 2019. 2
- [39] Xiangpeng Li, Jingkuan Song, Lianli Gao, Xianglong Liu, Wenbing Huang, Xiangnan He, and Chuang Gan. Beyond rnn: Positional self-attention with co-attention for video question answering. In *Proc. AAAI*, 2019. 2
- [40] Yingwei Li, Yi Li, and Nuno Vasconcelos. Resound: Towards action recognition without representation bias. In *Proc. ECCV*, 2018. 2, 6
- [41] Zhenyang Li, Kirill Gavriluk, Efstratios Gavves, Mihir Jain, and Cees G.M. Snoek. Videolstm convolves, attends and flows for action recognition. *Computer Vision and Image Understanding*, 166:41 – 50, 2018. 2
- [42] Junwei Liang, Lu Jiang, Liangliang Cao, Li-Jia Li, and Alexander G Hauptmann. Focal visual-text attention for visual question answering. In *Proc. CVPR*, 2018. 2
- [43] Ji Lin, Chuang Gan, and Song Han. Tsm: Temporal shift module for efficient video understanding. In *Proc. ICCV*, 2019. 2, 6, 14
- [44] Y. Liu, S. Albanie, A. Nagrani, and A. Zisserman. Use what you have: Video retrieval using representations from collaborative experts. In *Proc. BMVC*. 2
- [45] Chenxu Luo and Alan Yuille. Grouped spatial-temporal aggregation for efficient action recognition. In *Proc. ICCV*, 2019. 6, 8, 14, 18
- [46] Antoine Miech, Jean-Baptiste Alayrac, Lucas Smaira, Ivan Laptev, Josef Sivic, and Andrew Zisserman. End-to-end learning of visual representations from uncurated instructional videos. In *Proc. CVPR*, 2020. 2, 17
- [47] Antoine Miech, Ivan Laptev, and Josef Sivic. Learnable pooling with context gating for video classification. *arXiv preprint arXiv:1706.06905*, 2017. 2, 5, 7
- [48] Antoine Miech, Dimitri Zhukov, Jean-Baptiste Alayrac, Makarand Tapaswi, Ivan Laptev, and Josef Sivic. Howto100m: Learning a text-video embedding by watching hundred million narrated video clips. In *Proc. ICCV*, 2019. 2
- [49] Dian Shao, Yue Zhao, Bo Dai, and Dahua Lin. Finegym: A hierarchical video dataset for fine-grained action understanding. In *Proc. CVPR*, 2020. 2, 5, 6, 8, 14
- [50] Gunnar A Sigurdsson, Santosh Divvala, Ali Farhadi, and Abhinav Gupta. Asynchronous temporal fields for action recognition. In *Proceedings of the IEEE Conference on Computer Vision and Pattern Recognition*, pages 585–594, 2017. 15

- [51] Gunnar A Sigurdsson, Gül Varol, Xiaolong Wang, Ali Farhadi, Ivan Laptev, and Abhinav Gupta. Hollywood in homes: Crowdsourcing data collection for activity understanding. In *Proc. ECCV*, 2016. [2](#), [9](#), [14](#)
- [52] Karen Simonyan and Andrew Zisserman. Two-stream convolutional networks for action recognition in videos. In *Proc. NeurIPS*, 2014. [2](#)
- [53] Khurram Soomro, Amir Roshan Zamir, and Mubarak Shah. Ucf101: A dataset of 101 human actions classes from videos in the wild. *arXiv preprint arXiv:1212.0402*, 2012. [2](#)
- [54] Chen Sun, Fabien Baradel, Kevin Murphy, and Cordelia Schmid. Learning video representations using contrastive bidirectional transformer. *arXiv preprint arXiv:1906.05743*, 2019. [2](#)
- [55] Chen Sun, Austin Myers, Carl Vondrick, Kevin Murphy, and Cordelia Schmid. Videobert: A joint model for video and language representation learning. In *Proc. ICCV*, 2019. [2](#)
- [56] Yongyi Tang, Xing Zhang, Lin Ma, Jingwen Wang, Shaoliang Chen, and Yu-Gang Jiang. Non-local netvlad encoding for video classification. In *Proc. ECCV*, 2018. [2](#), [5](#), [7](#)
- [57] Yonglong Tian, Dilip Krishnan, and Phillip Isola. Contrastive multiview coding. *arXiv preprint arXiv:1906.05849*, 2019. [5](#)
- [58] Du Tran, Heng Wang, Lorenzo Torresani, Jamie Ray, Yann LeCun, and Manohar Paluri. A closer look at spatiotemporal convolutions for action recognition. In *Proc. CVPR*, 2018. [18](#)
- [59] George Turin. An introduction to matched filters. *IRE transactions on Information theory*, 6(3):311–329, 1960. [2](#)
- [60] Gül Varol, Ivan Laptev, and Cordelia Schmid. Long-term temporal convolutions for action recognition. *IEEE Transactions on Pattern Analysis and Machine Intelligence*, 40(6):1510–1517, 2018. [2](#)
- [61] Ashish Vaswani, Noam Shazeer, Niki Parmar, Jakob Uszkoreit, Llion Jones, Aidan N Gomez, Łukasz Kaiser, and Illia Polosukhin. Attention is all you need. In *Proc. NeurIPS*, 2017. [1](#), [2](#), [3](#), [6](#), [14](#), [17](#)
- [62] Heng Wang, Du Tran, Lorenzo Torresani, and Matt Feiszli. Video modeling with correlation networks. In *Proc. CVPR*, 2020. [6](#), [18](#)
- [63] Jinpeng Wang, Yiqi Lin, Andy J. Ma, and Pong C. Yuen. Self-supervised temporal discriminative learning for video representation learning. *arXiv preprint arXiv:2008.02129*, 2020. [5](#)
- [64] Limin Wang, Yuanjun Xiong, Zhe Wang, Yu Qiao, Dahua Lin, Xiaoou Tang, and Luc Van Gool. Temporal segment networks: Towards good practices for deep action recognition. In *Proc. ECCV*, 2016. [2](#), [6](#), [14](#), [18](#)
- [65] Xiaolong Wang, Ross Girshick, Abhinav Gupta, and Kaiming He. Non-local neural networks. In *Proc. CVPR*, 2018. [2](#), [15](#)
- [66] Xiaolong Wang and Abhinav Gupta. Videos as space-time region graphs. In *Proceedings of the European conference on computer vision (ECCV)*, pages 399–417, 2018. [15](#)
- [67] Michael Wray, Diane Larlus, Gabriela Csurka, and Dima Damen. Fine-grained action retrieval through multiple parts-of-speech embeddings. In *Proc. ICCV*, 2019. [2](#)
- [68] Chao-Yuan Wu, Christoph Feichtenhofer, Haoqi Fan, Kaiming He, Philipp Krahenbuhl, and Ross Girshick. Long-term feature banks for detailed video understanding. In *Proc. CVPR*, 2019. [2](#), [5](#), [7](#), [14](#), [15](#)
- [69] Jianchao Wu, Zhanghui Kuang, Limin Wang, Wayne Zhang, and Gangshan Wu. Context-aware rnn: A baseline for action detection in videos. In *Proc. ECCV*, 2020. [5](#)
- [70] Zhirong Wu, Yuanjun Xiong, Stella X Yu, and Dahua Lin. Unsupervised feature learning via non-parametric instance discrimination. In *Proc. CVPR*, 2018. [4](#), [5](#)
- [71] Tong Xiao, Shuang Li, Bochao Wang, Liang Lin, and Xiaogang Wang. Joint detection and identification feature learning for person search. In *Proc. CVPR*, 2017. [4](#), [5](#)
- [72] Saining Xie, Chen Sun, Jonathan Huang, Zhuowen Tu, and Kevin Murphy. Rethinking spatiotemporal feature learning: Speed-accuracy trade-offs in video classification. In *Proc. ECCV*, 2018. [2](#), [3](#), [5](#), [6](#), [7](#), [8](#), [14](#), [17](#)
- [73] Ruibin Xiong, Yunchang Yang, Di He, Kai Zheng, Shuxin Zheng, Chen Xing, Huishuai Zhang, Yanyan Lan, Liwei Wang, and Tie-Yan Liu. On layer normalization in the transformer architecture. In *Proc. ICML*, 2020. [6](#)
- [74] Ceyuan Yang, Yinghao Xu, Bo Dai, and Bolei Zhou. Video representation learning with visual tempo consistency. In *arXiv preprint arXiv:2006.15489*, 2020. [5](#)
- [75] Ceyuan Yang, Yinghao Xu, Jianping Shi, Bo Dai, and Bolei Zhou. Temporal pyramid network for action recognition. In *Proc. CVPR*, 2020. [2](#)
- [76] Yunan Ye, Zhou Zhao, Yimeng Li, Long Chen, Jun Xiao, and Yueting Zhuang. Video question answering via attribute-augmented attention network learning. In *Proceedings of the 40th International ACM SIGIR conference on Research and Development in Information Retrieval*, 2017. [2](#)
- [77] Joe Yue-Hei Ng, Matthew Hausknecht, Sudheendra Vijayanarasimhan, Oriol Vinyals, Rajat Monga, and George Toderici. Beyond short snippets: Deep networks for video classification. In *Proc. CVPR*, 2015. [2](#)
- [78] Chiyuan Zhang, Samy Bengio, Moritz Hardt, Benjamin Recht, and Oriol Vinyals. Understanding deep learning requires rethinking generalization. In *Proc. ICLR*, 2017. [18](#)
- [79] Zhou Zhao, Xinghua Jiang, Deng Cai, Jun Xiao, Xiaofei He, and Shiliang Pu. Multi-turn video question answering via multi-stream hierarchical attention context network. In *IJ-CAI*, 2018. [2](#)
- [80] Bolei Zhou, Alex Andonian, Aude Oliva, and Antonio Torralba. Temporal relational reasoning in videos. In *Proc. ECCV*, 2018. [2](#), [6](#), [14](#), [15](#), [18](#)
- [81] Linchao Zhu and Yi Yang. Actbert: Learning global-local video-text representations. In *Proc. CVPR*, 2020. [2](#)

# Appendices

## A. Visualization of Action Attention

In Figures 7 and 8 below, we show some samples with the predicted temporal attention by queries. Figure 7 shows some visualizations from Diving48, it can be seen that the attention for ‘take off’ is usually located at the beginning of the sequence, while the ones for the queries ‘turn’ and ‘twist’ span over multiple central clips. Figure 8 shows examples taken from FineGym, despite the variance between videos, the model always responds to ‘pose’ and ‘circle’ at the beginning of the action, while to ‘turn’ and ‘stand’ towards the end of the action.

Please refer to our project page<sup>1</sup> for visualizations using motion clips (GIFs).

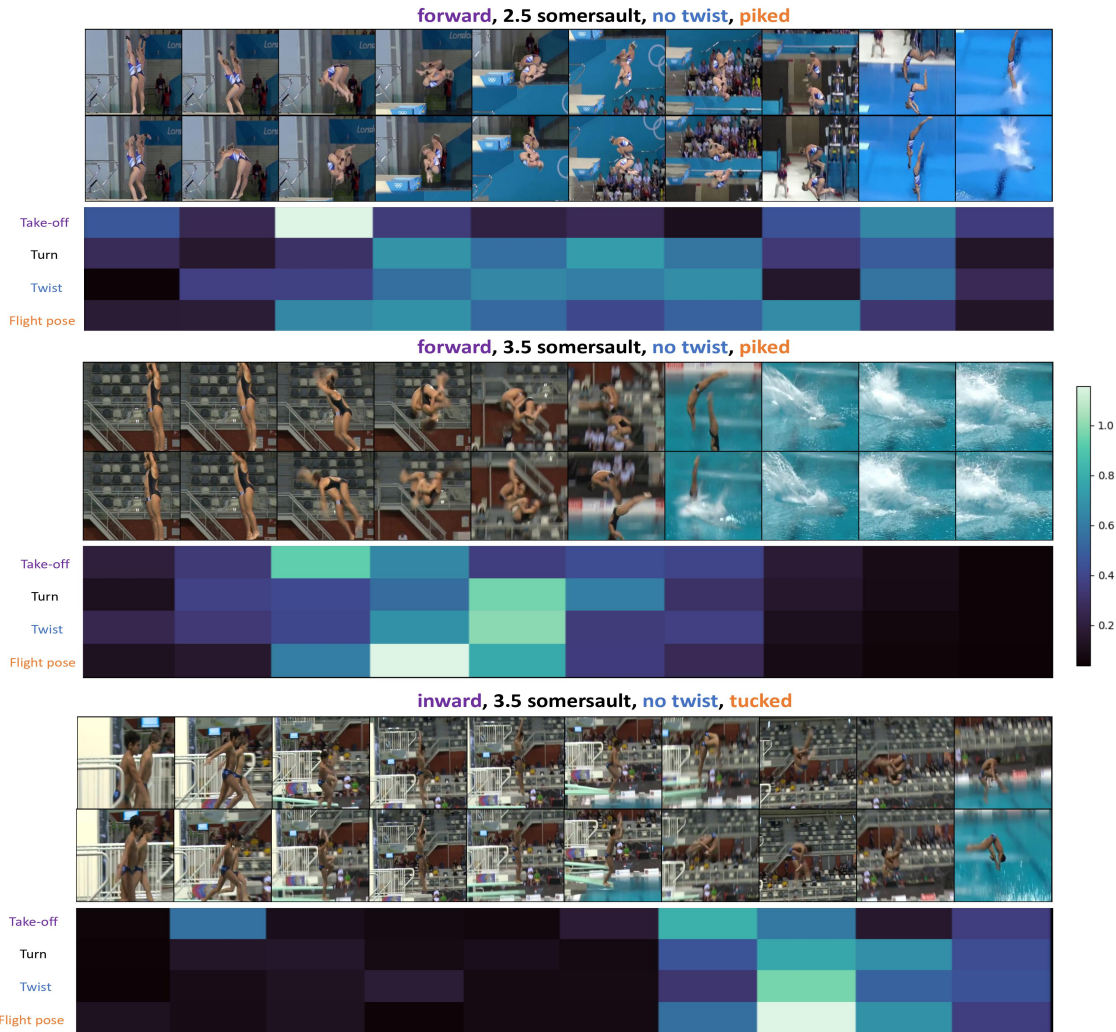


Figure 7: **Visualization of temporal attention from four queries in Diving48.** For every video sample, we show the attention scores over 10 clips from 4 queries by a 4x10 heatmap. Every clip contains 8 frames originally, here we show two from each (one above the other) for visualization.

<sup>1</sup><https://www.robots.ox.ac.uk/~vgg/research/tqn/>

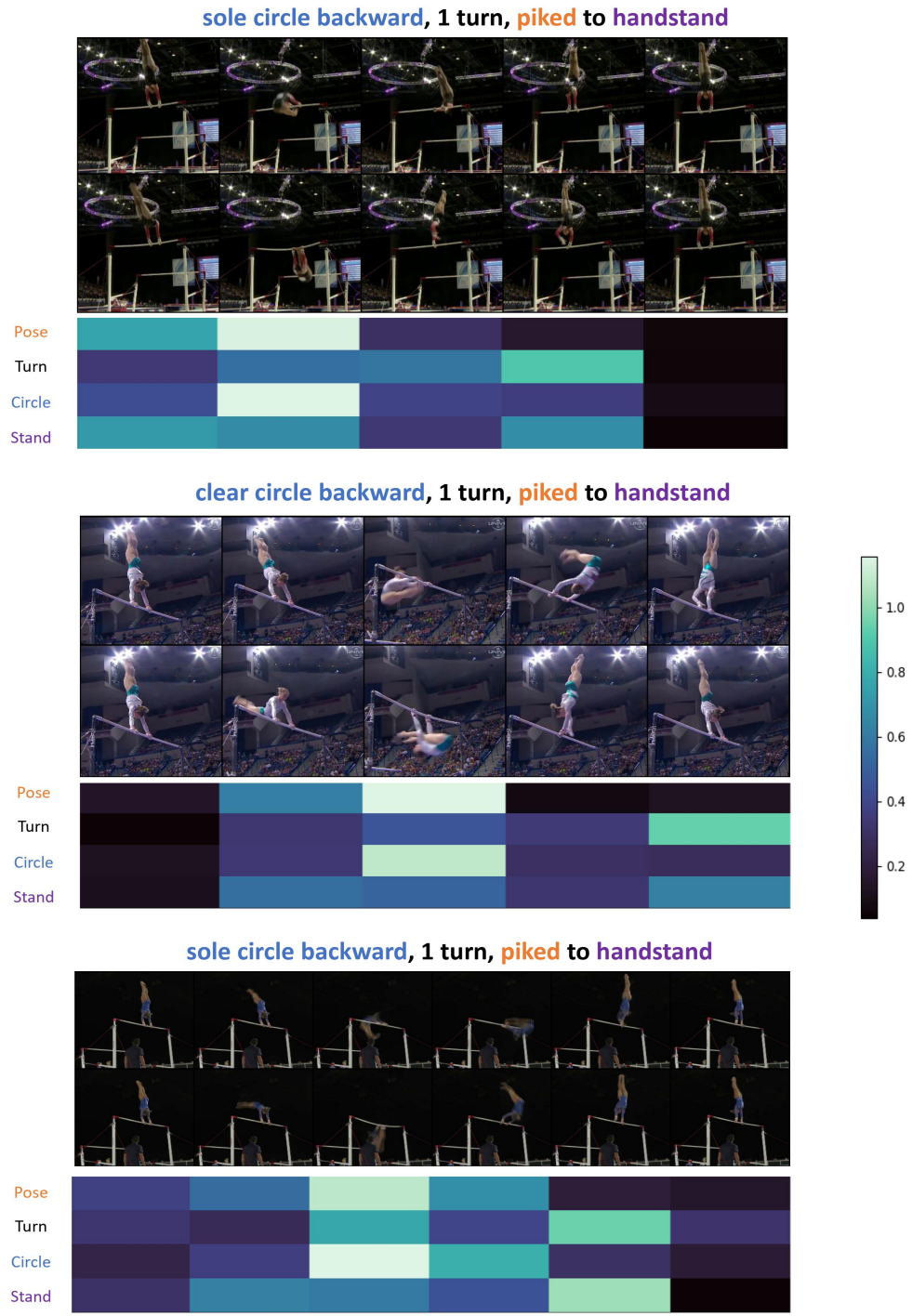


Figure 8: **Visualization of temporal attention from four queries in Gym99.** For every video sample, we show the attention scores over 5 clips from 4 queries by a 4x5 heatmap. Every clip contains 8 frames originally, here we show two from each (one above the other) for visualization.

Network	Pretrained dataset	Modality	# frames in training	Gym99				Gym288		Diving48	
				per-class	per-video			per-class	per-video	per-class	per-video
					subset VT	subset FX	total				
I3D [6]	K400	RGB	8	64.4	47.8	60.2	75.6	28.2	66.7	33.2	48.3
TSN [64]	ImageNet	RGB	3	68.7	46.6	72	74.8	26.5	68.3	26.9	41.3
	ImageNet	flow	3	77.2	42.6	81.2	84.7	38.7	78.3	28.1	38.8
TSM [43]	ImageNet	two-stream	3	79.8	47.5	84.6	86	37.6	79.9	34.8	52.5
	ImageNet	RGB	3	70.6	42.2	68.8	80.4	34.8	73.5	25.3	38.0
	ImageNet	flow	3	80.3	42.4	81.9	87.1	46.8	81.6	25.3	39.5
	ImageNet	two-stream	3	81.2	44.8	84.9	88.4	46.5	83.1	32.7	51.1
TRNms [80]	ImageNet	RGB	3	68.8	46.6	73.4	79.5	32.0	73.1	43.8	56.8
	ImageNet	flow	3	77.6	43.9	81.1	85.5	43.4	79.7	46.4	54.6
	ImageNet	two-stream	3	80.2	47.3	84.9	87.8	43.3	82.0	54.4	66.0
GST-50 [45]	ImageNet	RGB	8	84.6	53.6	84.9	89.5	46.9	83.8	69.5	78.9
ST-S3D [72]	K400	RGB	8	72.9	45.3	82.8	81.5	42.4	75.8	36.3	50.6
LT-S3D	K400	RGB	dense	88.9	69.1	90.4	92.5	57.9	86.3	72.3	80.4
TQN	K400	RGB	dense	<b>90.6</b>	<b>74.9</b>	<b>91.6</b>	<b>93.8</b>	<b>61.9</b>	<b>89.6</b>	<b>74.5</b>	<b>81.8</b>

Table 7: Full Comparison to SotA results on Gym99, Gym288, Diving48. with breakdown for RGB and flow.

## B. Full SotA Comparison

In FineGym [49], SotA baselines like TSN [64], TSM [43] and TRN [80] are trained using both RGB and flow. Due to space limitations, in Table 3 in the main paper we show only the best two-stream results from these model, without breakdown for RGB and flow. In Table 7 the detailed breakdown is shown: although the performance from two-streams is better than using only one modality for previous work, our model achieves superior results to all of these using only RGB frames.

## C. Extension to Multi-label Action Recognition

We apply TQN to the Charades dataset [51] and evaluate its performance on multi-label action recognition. Results are shown in Table 8.

Charades contains 9.8k training and 1.8k test crowd-sourced videos (avg. length: 30 secs) of scripted indoor activities, with each video containing one or more actions (avg. duration = 12 secs/action) out of 157 total different action classes. As opposed to classification in FineGym and Diving48 where a sequence of combined actions are labelled as one class without localization, Charades labels multiple actions in one video as different classes with precise temporal annotations.

Since the action classes in Charades do not form any natural clustering, we treat each class as an individual query and train the TQN to make binary classification. More specifically, the 157 learnable queries corresponds to 157 classes, and their output predict whether these actions exist or not. For training, we follow two-stage training pipeline in [68]. In the first stage, we train the model on clips of 3.2 seconds to make clip-level prediction. In the second stage, we add in the stochastically updated feature bank to train the model for video-level prediction with dense features sampled from the entire video sequence.

During inference, we follow [68] and use 3-crop test to evaluate two models: 1) The model trained without stochastically updated feature bank in the 1st stage. This model makes clip-level predictions which are aggregated by maxpooling to output video-level predictions. 2) The model trained with stochastically updated feature bank using two-stage training.

Results in Table 8 show that when trained on short clips, the TQN architecture is better than most of the other architectures. When the stochastically updated feature bank is used in training, the performance is further improved, leading to a better mAP compared to others using the same visual backbone pretrained on Kinetics-400.

## D. Implementation Details

**Decoder architecture.** The decoder has the same architecture as a basic Transformer decoder [61]. The decoder takes features from the visual encoder for keys and values, and the learnt embeddings as queries. In every attention layer, the decoder attends to keys and aggregate the values to update the queries. The updated queries serve as new input queries to the next layer which interact with visual features in the same way. Linear classifiers are applied to the output features from the decoder for attribute prediction.

In our experiments on FineGym and Diving48, we use four attention layers with four heads with 1024 feed-forward dimension, with dropout rate equal to 0.1 in the decoder and 0.5 for output features. In our experiments on Charades, we use two attention layers with two heads with 1024 feed-forward dimension, with dropout rate equal to 0.1 in the decoder and 0.3 for output features. We omit positional encoding in all the experiments as we find it leads to overfitting in this task.

**Data augmentation.** The input images are non-overlapping contiguous video clips of 8 frames with temporal stride of 1 in FineGym, 8 frames with temporal stride of 2 in Diving48 and 32 frames with temporal stride of 4 in Charades. In all the training, we apply color

	Backbone	Feature bank	Pretrain	Train/val
Asyn-TF [50]	VGG16	✗	ImageNet	22.4
TRNms [80]	Inception	✗	ImageNet	25.2
I3D [6] (from [65])	R101-I3D	✗	K400	35.5
I3D-NL [65] (from [68])	R50-I3D-NL	✗	K400	37.5
STRG [66]	R50-I3D-NL	✗	K400	37.5
STO [68]	R50-I3D-NL	✗	K400	39.6
LFB NL [68]	R50-I3D-NL	✓	K400	40.3
TQN	R50-I3D-NL	✗	K400	40.7
TQN	R50-I3D-NL	✓	K400	<b>41.4</b>
STO [68]	R101-I3D-NL	✗	K400	41.0
SlowFast NL [15]	R101-I3D-NL	✗	K400	42.5
LFB NL [68]	R101-I3D-NL	✓	K400	42.5
TQN	R101-I3D-NL	✗	K400	42.1
TQN	R101-I3D-NL	✓	K400	<b>42.9</b>
SlowFast NL [15]	R101-I3D-NL	✗	K600	45.2

Table 8: Comparison to state-of-the-art on Charades when using temporal localization.

Dataset	1st stage			2nd stage		
	# epochs	sequence shorter than N frames	lr multiplier	# epochs	sequence shorter than N frames	lr multiplier
FineGym	50	48	1	35	max (all videos)	0.1 @ epoch 10 ,
Diving48	50	128	1	35	max (all videos)	0.01 @ epoch 20
Charades	50	128	0.1 @ epoch 35 , 0.01 @ epoch 45	35	max (all videos)	0.1 @ epoch 6

Table 9: Details of multi-stage training with stochastic feature bank on different datasets.

jittering (brightness factor  $\in [0.6, 1.4]$ , contrast factor  $\in [0.3, 1.7]$ , saturation factor  $\in [0.3, 1.7]$ , hue  $\in [-0.25, 0.25]$ ) and horizontal flips (with probability 50%) on images of size 224 x 224 pixel.

In training of FineGym and Diving, we apply spatial and temporal augmentation. In the spatial dimension, we randomly crop the frames to squares of 60%-100% of the original height, and resize them to 224x224 pixels. In the temporal dimension, we randomly remove 2% of frames when sampling as augmentation. In training of Charades, we follow the random spatial crop in [68] without further temporal augmentation.

**Inference.** When testing TQN, all the features from one video are computed online without using the feature bank.

When TQN is tested on FineGym and Diving, only center-crops are used. For every sample, we randomly remove 2% of frames three times to obtain three sequences, and average the class probabilities from them to obtain final predictions. For other baseline models which are trained on a fixed number of frames but tested with all frames (*e.g.*, ablation studies in Section 5.2 in the main paper), we use multiple clips in inference. We randomly/consecutively sample multiple clips (with the same number of frames per clip as in training) so that they cover the full video sequence, and average the class probabilities from all the clips to obtain final predictions.

On Charades, we follow [65] and use 3 spatial crops for each clip in inference without temporal jittering. The predictions from 3 crops are aggregated by maxpooling the class probabilities.

**Learning rate schedule.** For FineGym and Diving48, no temporal localization information is used in the training. Our training pipeline contains two stages: (1) end-to-end training on short videos as warm-up to obtain a good initialization. (2) Training with a stochastically updated memory feature bank on the longer videos in a bootstrapping way.

we use Adam optimizer with base learning rate 0.001 in the encoder and 0.0001 in the decoder, and the weight decay is 1e-5. For Charades, we use SGD optimizer with base learning rate 0.02 with momentum 0.9, weight decay is set to 1.25e-5. Detailed schedule of training is shown in Table 9.

When temporal localization is used in training (Charades), we first use the localization to train the model to do clip-level actions as in [68] for 45 epochs with learning rate 0.01 decreased by 10 at epoch 35, and then use stochastically updated memory feature bank to train the model to make video-level actions using learning rate 0.01 for 16 epochs, decreased by 10 at epoch 6.

**Feature bank.** Before we use the feature bank, we first train the model end-to-end on videos shorter than  $N$  clips (detailed in table 9). We use this model to initialize the feature bank: feature vectors from all training videos are extracted and cached. The feature bank storage takes 452Mb for Charades, 725Mb for Diving48, 871Mb for Gym99, and 1.5G for Gym288 (40k training videos, 6 clips in each video on average). During training with the stochastically updated feature bank, at each iteration, features from  $n_{\text{online}}$  randomly selected contiguous clips are computed online and cached in the bank;  $n_{\text{online}} = 10$  in Diving48,  $n_{\text{online}} = 6$  in FineGym, and  $n_{\text{online}} = 3$  in Charades. For inference, all the features from one video are computed online without using a feature bank.

## E. Ablation on Two-Stage Training

We adapt the two-stage training to obtain good performance on long videos. In the warm-up stage where the model is trained end to end efficiently on short videos with the number of clips up to  $k_{\text{first}}$ , where 1 clip spans over 16 frames, with temporal downsampling rate equal to 2. And in the second stage we train the model with the feature bank on the whole dataset containing both short and long videos. In every iteration, we compute features from  $n_{\text{online}}$  clips online and update them in the feature bank. Here we ablate how the choice of  $k_{\text{first}}$  and  $n_{\text{online}}$  affects the final performance.

We use  $k_{\text{first}} = 8$  and  $n_{\text{online}} = 10$  in all the experiments presented in the main paper. In the following experiments, we use change one of them to different values and keep the other fixed, and use the Diving48 dataset for evaluation.

In Table 10, we have  $k_{\text{first}} \in \{0, 4, 6, 8\}$  and keep  $n_{\text{online}}$  constant as 10. When  $k_{\text{first}}$  there is no warm-up training, we use the model pre-trained on Kinetics400 [30] as initialization and train with the feature bank directly, the per class and per videos accuracy is 72.3% and 79.2% respectively. When warm-up training is done on videos shorter than 4 clips, it actually worsens the performance, as such videos only account for 5% of the whole dataset, resulting in overfitting. When  $k_{\text{first}}$  is further increased to 8, it gives improvement on both per-video and per-class accuracy by 2%.

In Table 11, we keep  $k_{\text{first}}$  fixed as 8 and increase  $n_{\text{online}}$  from 0 to 10 (0 meaning no 2nd stage training using memory banks). Increasing the size of  $n_{\text{online}}$  also gives better performance. Both per-class accuracy and per-video accuracy is improved by 2% when  $n_{\text{online}}$  is doubled from 4 to 8.

Therefore, both two stages are necessary to obtain good results. In the first stage the model is trained efficiently on short videos. It prevents the model from overfitting to uninformative clips in the second stage, especially when a small number of clips are updated online. The second stage makes it possible to train the model on long sequences which are impossible to fit into first stage. We use two RTX 6000 GPUs (total 48 GB memory) in our main experiments, if more GPU memory is available,  $k_{\text{first}}$  and  $n_{\text{online}}$  could be increased to even higher numbers for better performance.

Use videos up to $k_{\text{first}}$ clips in warm-up training	Accuracy	
	per class	per video
$k_{\text{first}} = 8$	74.5	81.8
$k_{\text{first}} = 6$	69.4	79.7
$k_{\text{first}} = 4$	67.5	78.9
$k_{\text{first}} = 0$	72.3	79.2

Table 10: Ablation of max length of videos used in warm-up training (the 1st stage in 2-stage training).

$n_{\text{online}}$ clips updated in feature bank	Accuracy	
	per class	per video
$n_{\text{online}} = 10$	74.5	81.8
$n_{\text{online}} = 8$	71.1	80.3
$n_{\text{online}} = 6$	70.4	79.7
$n_{\text{online}} = 4$	69.8	78.3
$n_{\text{online}} = 0$	64.4	75.8

Table 11: Ablation of number of clips updated in the feature bank (the 2nd stage in 2-stage training).

## F. Feature Bank vs. End-to-end Training

To benchmark how closely the stochastically updated feature bank can approximate the ideal end-to-end training, we investigate the performance gap between the two settings. Comparisons are done on videos shorter than 16 clips (256 frames) in Diving48 so that the full sequence can fit into memory of four RTX 6000 (96GB total) (we use two extra GPUs here for benchmarking feature banks; all other experiments use two GPUs due to limited budget). The training pipeline is the same as the one in the main paper except the 1st stage training is done on videos shorter than 8 clips instead of 10 clips here (as the max length of videos are now smaller).

The first three rows in Table 12 show the results from using the stochastically updated feature bank, with different update step sizes in one iteration. The last row shows the results from end-to-end training with densely sampled frames from the whole video. The gap between updating 12 clips (75% of max length) and end-to-end training is less than 1%. Hence, with good initialization and large update step, the performance from using the feature bank can be close to the one from end-to-end training.

In our experiments in Diving48 in the main paper, our update step size is 10 clips (160 frames, 50% of the max length). The accuracy (81.8% per video) might be further improved with more GPU memory and larger step size.

Method	# clips updated in feature bank	Accuracy	
		per-class	per-video
Feature bank	4	70.2	79.3
	8	71.7	81.3
	12	73.0	81.4
End-to-End	-	73.9	81.6

Table 12: Performance gap between training with the feature bank and end-to-end training. Comparison is done on videos shorter than 256 frames so that end-to-end training is possible with our memory capacity.



## G. Text Supervision

In Section 5.1 in the main paper, we explore different ways of leveraging multi-attribute labels, and compare them to standard multi-class classification on Diving48, the results are reproduced in Table 13. Here we describe the details of all the methods and their architectures, and analyze their performance on fine-grained action recognition. For fair comparison, we use S3D as the visual encoder for all the architectures below. When a Transformer encoder or decoder is used in the method, we construct them with 4 attention layers and 4 attention heads so that their number of parameters is similar or the same as our TQN decoder.

Backbone	Encoder	Decoder (Aggregation)	Classification	Label	Accuracy	
					per-class	per-video
S3D	–	average pooling	multi-class (cross entropy)	class index	72.3	80.4
	self-attention	–	multi-label (binary cross entropy)		text	47.9
		auto-regressive Transformer	sequence prediction (cross entropy)	descriptions	51.9	65.1
		–	TQN		multi-task (cross entropy)	74.5

Table 13: **Leveraging multi-part text descriptions.** We compare our *query-attribute* label factorization to alternative methods for learning with unaligned (no temporal location information) multi-part text descriptions on the Diving48 dataset.. Our TQN + label factorization outperforms other approaches which are representative of standard classification, and modern encoder-decoder architectures for sequences.

**1. S3D + Average pooling, standard multi-class classification, cross-entropy loss.** When only class indices are given as supervision, the most standard way is to do classification directly on aggregated temporal features [6, 14, 72]. Therefore, we use a S3D without any Transformer encoder/decoder, and average pool the output features from it, apply 0.5 dropout and a linear classifier on it for 48-way classification in Diving48. It acts as a strong baseline with 72.3% per-class accuracy and 80.4% per video accuracy .

**2. S3D + TFM encoder, standard multi-class classification, cross-entropy loss.** For context aggregation we add a transformer on top of visual encoder before temporal average pooling as in model (1). We follow the common practice in [12, 13] and append a learnable ‘cls’ token to the visual features as input to the Transformer encoder, the output of this token is trained to do 48-way classification with cross-entropy loss. With a self-attention encoder to model long-term temporal information, the per-class accuracy is increased by 1.4% compared to S3D + average pooling (*i.e.*, model (1) above).

**3. S3D + TFM encoder, multi-label classification, binary cross-entropy loss.** Multi-label classification uses  $K$  binary classifiers, one for each attribute, with  $M$  annotations for each sample. We use the attributes from our query-attributes factorization (Section 3.3 in the main paper) as ground-truth labels, hence  $K$  is the total number of attributes (possible query answers), and  $M$  is the number of ground-truth labels per video, which is fixed and equal to the number of queries in the dataset.

Unlike TQN which has multiple experts to predict an answer to each query individually, labels in multi-label classification are usually predicted by one linear head. Again, we use an S3D with a Transformer encoder, and append a learnable ‘cls’ token to the visual features as input to the Transformer encoder. The output from the ‘cls token’ is trained with binary cross entropy to predict multiple labels.

For a given video, we map the probabilities of predicted attributes  $P_{\text{att}} \in \mathbb{R}^K$  to class probabilities. The probability  $P_{\text{class}}^{(i)} \in \mathbb{R}$  of a certain class  $i$ , is computed by aggregating the joint probability over the  $M$  pre-defined attributes  $\mathcal{L}_i \subset \{1, 2, \dots, K\}$ ,  $|\mathcal{L}_i| = M$  (out of total  $K$  predicted) for that class:

$$P_{\text{class}}^{(i)} = \prod_{j \in \mathcal{L}_i} P_{\text{att}}^{(j)}. \quad (3)$$

Note,  $i$  ranges over  $k_{\text{first}}$  originally defined fine-grained action categories (*e.g.*,  $k_{\text{first}} = 8$  in Diving48).  $P_{\text{att}}^{(j)}$  is the probability of  $j$ th attribute out of total  $K$  attributes. The final class prediction is taken as the argmax value of  $P_{\text{class}}$ .

It turns out that with a single head, it is hard to predict different attributes of the action accurately, per-video accuracy of this model is 25% lower than that of multi-class classification models (1) and (2).

**4. S3D + TFM decoder, sequence prediction, cross-entropy loss.** Sequence prediction is another popular way to learn video representation from texts [11, 12, 46]. We follow the original Seq2Seq architecture in [61], and use a transformer decoder which takes visual features as input and decodes the sequence in an autoregressive manner. We use the attributes from our query-attributes factorization, and assemble the ground-truth attributes for every sample as the ground-truth sequence. To map the sequence prediction  $y_{\text{seq}}$  to class prediction, we compute its edit distance to the ground-truth sequence, the one with smallest edit distance is treated as the predicted class.

$$P_{\text{class}} = \arg \min_i (\text{EditDist}(y_{\text{seq}}, \text{GT}_i)) \quad (4)$$

In a Seq2Seq model, prediction at one step is made dependent on the output of previous steps, which is ideal for language with grammar, but not for discretized and independent action types in our task. It leads to worse generalization ability at inference time, with per-video accuracy 16% lower than that of TQN.

## H. Comparison to SotA Results on Diving48-v1 (the noisy version)

There are two versions of Diving48: Diving48-v1(Aug 2018) is the early and noisy version where 43.5% of training, and 35.8% of test videos were mislabelled; the newly released Diving48-v2(Oct 2020) has all the mislabelled data corrected. We find it is hard to interpret previous results [28, 62] on Diving48-v1 given heavy label noise, hence comparison on Diving48-v2 are reported in the main paper instead.

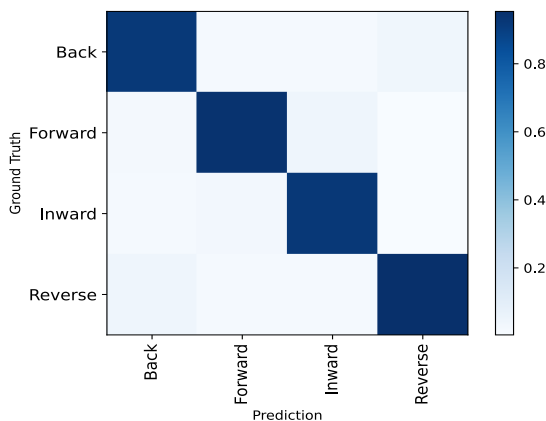
Here we include the SotA comparison on Diving48-v1 for completeness in Table 14. On this version, we report results from our baseline Long-term S3D(LT-S3D) and TQN. The use of query decoder has shown 2% improvement over the baseline, and ranks as the second in the comparison. The best result is from the deepest network CorrNet-101 [62] pre-trained on dataset Sports1M [29] 6 times larger than Kinetics400 [30]. Its backbone has 101 layers, which is about 4 times deeper than ours. On a heavily mislabelled dataset, it is hard to deduce whether the advantage comes from better action understanding or the fact that large models overfit better to noise [78].

Network	modality	Pre-training	Per video Accuracy
TSN [64]	RGB	ImageNet	16.8
	RGB+Flow	ImageNet	20.3
TRN [80]	RGB+Flow	ImageNet	22.8
R(2+1)D [58]	RGB	Sports1M	28.9
DiMoFs [3]	RGB	Kinetics	31.4
Attention-LSTM [28]	RGB	ImageNet	35.6
GST-50 [45]	RGB	ImageNet	38.8
CorrNet-50 [62]	RGB	x	37.9
CorrNet-101 [62]	RGB	Sports1M	<b>44.7</b>
LT-S3D	RGB	K400	36.3
TQN	RGB	K400	38.9

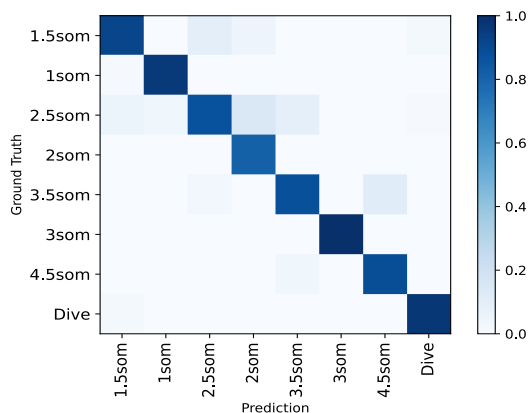
Table 14: Comparison to SoTA on the noisy version of Diving48.

## I. Error Analysis: Confusion Matrices

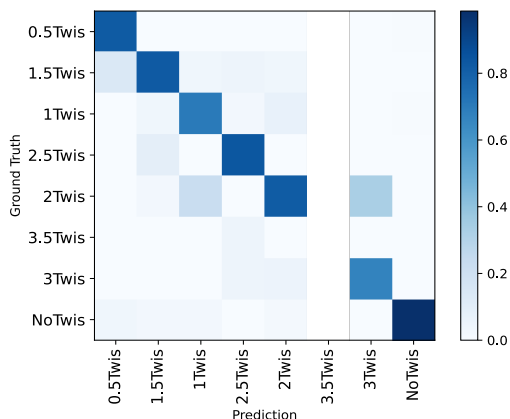
We visualize the confusion matrices from different queries to show the performance of TQN in distinguishing attributes associated with a query. Figure 9 shows confusion matrices for Diving48, and Figure 10 show those for Gym99. TQN does well in predicting pose-based attributes in ‘take off’, ‘flight pose’ and ‘position’. The main errors come from counting the number of turns and twists, especially those with similar counts. Because of unbalanced classes, it also has difficulty in learning attributes with very few training samples, e.g., the attribute ‘3.5Twis’ in the query ‘twist’ (Figure 9(c)) only accounts for 0.3% of the training data.



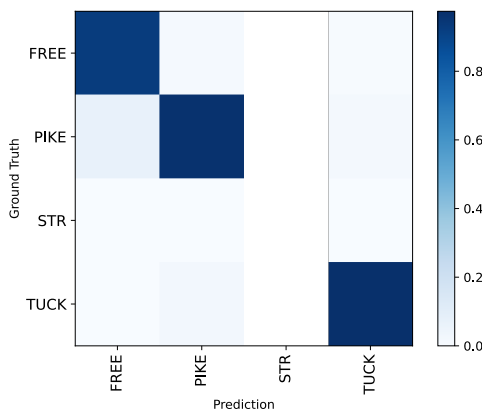
(a) Attributes to the query ‘take off’



(b) Attributes to the query ‘somersault’



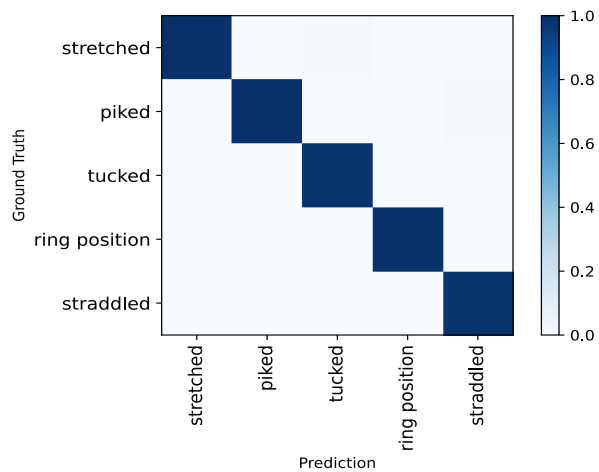
(c) Attributes to the query ‘twist’



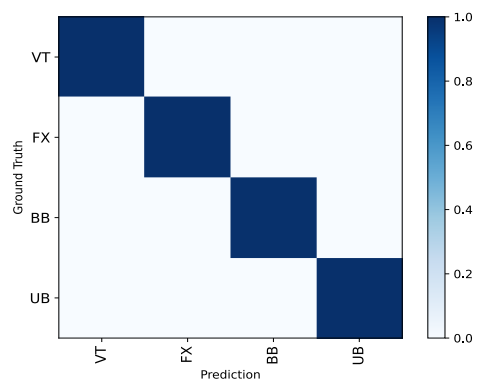
(d) Attributes to the query ‘flight pose’

Figure 9: Confusion matrix of attributes predicted by TQN to different queries on Diving48.

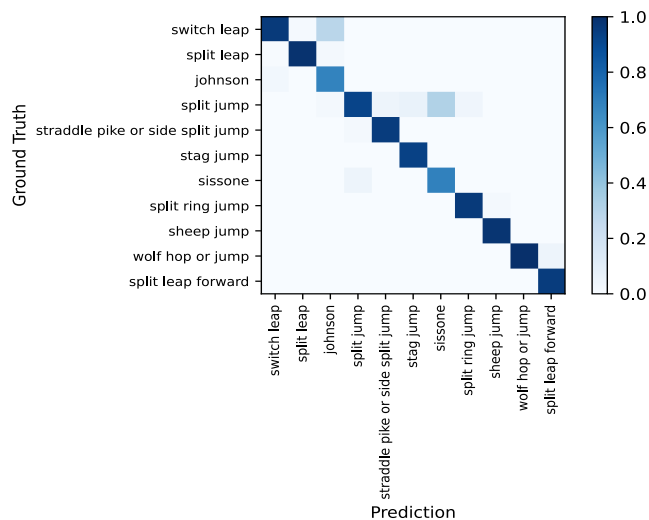
Figure 10: Confusion matrix of attributes predicted by TQN to different queries on Gym99.



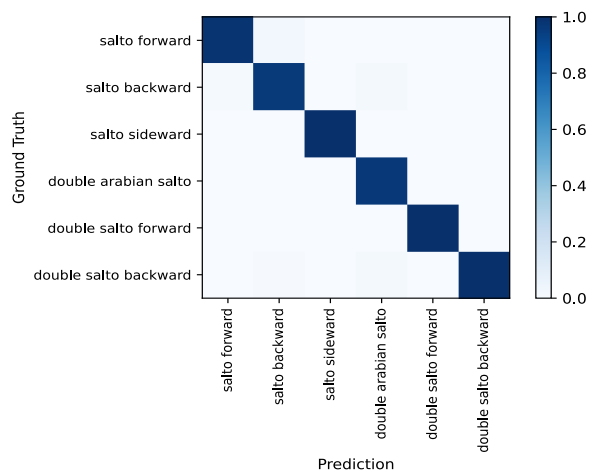
(a) Attributes to the query 'position'



(b) Attributes to the query 'event'



(c) Attributes to the query 'jump'



(d) Attributes to the query 'tumbling'

## J. Query-Attributes Specification

We show the complete query-attribute factorization for Diving48, Gym99 in full detail here, the details of Gym299 is attached as .csv files along with the supplementary material.

Table 15: List of queries and their possible responses (attributes) in Diving48.

q_id	q_name	att_id	att_name
-	-	0	null
0	take off	1	backward
		2	forward
		3	reverse
		4	inward
1	somersault	5	dive
		6	1 somersault
		7	1.5 somersault
		8	2 somersault
		9	2.5 somersault
		10	3 somersault
		11	3.5 somersault
		12	4.5 somersault
2	twist	13	no twist
		14	0.5 twist
		15	1.0 twist
		16	1.5 twist
		17	2.0 twist
		18	2.5 twist
		19	3 twist
		20	3.5 twist
3	flight pose	21	tucked
		22	piked
		23	straight
		24	free

Table 16: **Mapping of classes to their queries and responses in Diving48.** We show all the 48 classes in Diving48 and their responses to four queries: take off, somersault, twist and flight pose.

class index	class name	attribute id for each query			
		take off	somersault	twist	flight pose
0	Back,1.5som,05Twis,FREE	1	7	14	24
1	Back,1.5som,15Twis,FREE	1	7	16	24
2	Back,1.5som,25Twis,FREE	1	7	18	24
3	Back,1.5som,NoTwis,PIKE	1	7	13	22
4	Back,1.5som,NoTwis,TUCK	1	7	13	21
5	Back,2.5som,15Twis,PIKE	1	9	16	22
6	Back,2.5som,25Twis,PIKE	1	9	18	22
7	Back,2.5som,NoTwis,PIKE	1	9	13	22
8	Back,2.5som,NoTwis,TUCK	1	9	13	21
9	Back,2som,15Twis,FREE	1	8	16	24
10	Back,2som,25Twis,FREE	1	8	18	24
11	Back,3.5som,NoTwis,PIKE	1	11	13	22
12	Back,3.5som,NoTwis,TUCK	1	11	13	21
13	Back,3som,NoTwis,PIKE	1	10	13	22
14	Back,3som,NoTwis,TUCK	1	10	13	21
15	Back,Dive,NoTwis,PIKE	2	5	13	22
16	Back,Dive,NoTwis,TUCK	2	5	13	21
17	Forward,1.5som,1Twis,FREE	2	7	15	24
18	Forward,1.5som,2Twis,FREE	2	7	17	24
19	Forward,1.5som,NoTwis,PIKE	2	7	13	22
20	Forward,1som,NoTwis,PIKE	2	6	13	22
21	Forward,2.5som,1Twis,PIKE	2	9	15	22
22	Forward,2.5som,2Twis,PIKE	2	9	17	22
23	Forward,2.5som,3Twis,PIKE	2	9	19	22

class index	class name	attribute id for each query			
		take off	somersault	twist	flight pose
24	Forward,2.5som,NoTwis,PIKE	2	9	13	22
25	Forward,2.5som,NoTwis,TUCK	2	9	13	21
26	Forward,3.5som,NoTwis,PIKE	2	11	13	22
27	Forward,3.5som,NoTwis,TUCK	2	11	13	21
28	Forward,45som,NoTwis,TUCK	2	12	13	21
29	Forward,Dive,NoTwis,PIKE	2	5	13	22
30	Forward,Dive,NoTwis,STR	2	5	13	23
31	Inward,1.5som,NoTwis,PIKE	3	7	13	22
32	Inward,1.5som,NoTwis,TUCK	3	7	13	21
33	Inward,2.5som,NoTwis,PIKE	3	9	13	22
34	Inward,2.5som,NoTwis,TUCK	3	9	13	21
35	Inward,3.5som,NoTwis,TUCK	3	11	13	21
36	Inward,Dive,NoTwis,PIKE	3	5	13	22
37	Reverse,1.5som,05Twis,FREE	3	7	14	24
38	Reverse,1.5som,15Twis,FREE	3	7	16	24
39	Reverse,1.5som,25Twis,FREE	3	7	18	24
40	Reverse,1.5som,35Twis,FREE	3	7	20	24
41	Reverse,1.5som,NoTwis,PIKE	3	7	13	22
42	Reverse,2.5som,15Twis,PIKE	3	9	16	22
43	Reverse,2.5som,NoTwis,PIKE	3	9	13	22
44	Reverse,2.5som,NoTwis,TUCK	3	9	13	21
45	Reverse,3.5som,NoTwis,TUCK	3	11	13	21
46	Reverse,Dive,NoTwis,PIKE	3	5	13	22
47	Reverse,Dive,NoTwis,TUCK	3	5	13	21

Table 17: List of queries and their possible responses (attributes) in Gym99.

q_id	q_name	att_id	att_name
-	-	0	null
0	event	1	VT
		2	FX
		3	BB
		4	UB
1	onto	5	round-off
2	tumbling	6	salto forward
		7	salto backward
		8	salto sideward
		9	arabian salto
		10	double arabian salto
		11	double salto forward
12	double salto backward		
3	flic-flac	13	flic-flac
4	acrobatics	14	free aerial cartwheel
		15	walkover forward
5	jump	16	switch leap
		17	split leap
		18	johnson
		19	split jump
		20	straddle pike or side split jump
		21	stag jump
		22	sissonne
		23	split ring jump
		24	sheep jump
		25	wolf hop or jump
		26	split leap forward
		6	position
28	piked		
29	tucked		
30	ring position		
31	straddled		
7	turn	32	0.5 turn
		33	1 turn
		34	1.5 turn
		35	2 turn
		36	2.5 turn
		37	3 turn
		38	1.5 turn or more
		39	2 turn or more

q_id	q_name	att_id	att_name
8	twist	40	0.5 twist
		41	1 twist
		42	2 twist
		43	1.5 twist
		44	3 twist
		45	2.5 twist
9	circle	46	stalder backward
		47	sole circle backward
		48	giant circle backward
		49	giant circle forward
		50	clear circle backward
		51	clear hip circle backward
		52	counter over high bar
		53	swing forward
		54	swing backward
		55	transition flight from high bar to low bar
		56	transition flight from low bar to high bar
10	stand	57	free leg held upward in 180 split position throughout turn
		58	legs together
		59	on one leg free leg straight throughout turn
		60	on one leg free leg optional
		61	with heel of free leg forward at horizontal throughout turn
		62	landing on one or both feet
		63	step out
		64	take off from one leg to side stand
		65	handstand

Table 18: **Mapping of classes to their queries and responses in Gym99.** We show all the 99 classes in Gym99 and their responses to the 11 queries.

class id	class name	attribute id for each query										
		event	onto	tumbling	flic-flac	acrobatics	jump	position	turn	twist	circle	stand
0	round-off, flic-flac with 0.5 turn on, stretched salto forward with 0.5 turn off	1	0	6	13	0	0	27	32	0	0	0
1	round-off, flic-flac on, stretched salto backward with 2 turn off	1	5	7	13	0	0	27	35	0	0	0
2	round-off, flic-flac on, stretched salto backward with 1 turn off	1	5	7	13	0	0	27	33	0	0	0
3	round-off, flic-flac on, stretched salto backward with 1.5 turn off	1	5	7	13	0	0	27	34	0	0	0
4	round-off, flic-flac on, stretched salto backward with 2.5 turn off	1	5	7	13	0	0	27	36	0	0	0
5	round-off, flic-flac on, stretched salto backward off	1	5	7	13	0	0	27	0	0	0	0
6	switch leap with 0.5 turn	2	0	0	0	0	16	0	32	0	0	0
7	switch leap with 1 turn	2	0	0	0	0	16	0	33	0	0	0
8	split leap with 1 turn	2	0	0	0	0	17	0	33	0	0	0
9	split leap with 1.5 turn or more	2	0	0	0	0	17	0	0	38	0	0
10	switch leap (leap forward with leg change to cross split)	2	0	0	0	0	16	0	0	0	0	0
11	split jump with 1 turn	2	0	0	0	0	19	0	33	0	0	0
12	split jump (leg separation 180 degree parallel to the floor)	2	0	0	0	0	19	0	0	0	0	0
13	johnson with additional 0.5 turn	2	0	0	0	0	18	0	32	0	0	0
14	straddle pike or side split jump with 1 turn	2	0	0	0	0	20	0	33	0	0	0
15	switch leap to ring position	2	0	0	0	0	16	30	0	0	0	0
16	stag jump	2	0	0	0	0	21	0	0	0	0	0
17	2 turn with free leg held upward in 180 split position throughout turn	2	0	0	0	0	0	0	35	0	0	57
18	2 turn in tuck stand on one leg, free leg straight throughout turn	2	0	0	0	0	0	29	35	0	0	59
19	3 turn on one leg, free leg optional below horizontal	2	0	0	0	0	0	0	37	0	0	60
20	2 turn on one leg, free leg optional below horizontal	2	0	0	0	0	0	0	35	0	0	60
21	1 turn on one leg, free leg optional below horizontal	2	0	0	0	0	0	0	33	0	0	60
22	2 turn or more with heel of free leg forward at horizontal throughout turn	2	0	0	0	0	0	0	0	39	0	61
23	1 turn with heel of free leg forward at horizontal throughout turn	2	0	0	0	0	0	0	33	0	0	61
24	arabian double salto tucked	2	0	10	0	0	0	29	0	0	0	0
25	salto forward tucked	2	0	6	0	0	0	29	0	0	0	0
26	aerial walkover forward	2	0	0	0	15	0	0	0	0	0	0
27	salto forward stretched with 2 twist	2	0	6	0	0	0	27	0	42	0	0
28	salto forward stretched with 1 twist	2	0	6	0	0	0	27	0	41	0	0
29	salto forward stretched with 1.5 twist	2	0	6	0	0	0	27	0	43	0	0
30	salto forward stretched, feet land together	2	0	6	0	0	0	27	0	0	0	62
31	double salto backward stretched	2	0	12	0	0	0	27	0	0	0	0
32	salto backward stretched with 3 twist	2	0	7	0	0	0	27	0	44	0	0
33	salto backward stretched with 2 twist	2	0	7	0	0	0	27	0	42	0	0
34	salto backward stretched with 2.5 twist	2	0	7	0	0	0	27	0	45	0	0



Table 18: **Mapping of classes to their queries and responses in Gym99.** We show all the 99 classes in Gym99 and their responses to the 11 queries.

class id	class name	attribute id for each query										
		event	onto	tumbling	flic-flac	acrobatics	jump	position	turn	twist	circle	stand
35	salto backward stretched with 1.5 twist	2	0	7	0	0	0	27	0	43	0	0
36	double salto backward tucked with 2 twist	2	0	12	0	0	0	29	0	42	0	0
37	double salto backward tucked with 1 twist	2	0	12	0	0	0	29	0	41	0	0
38	double salto backward tucked	2	0	12	0	0	0	29	0	0	0	0
39	double salto backward piked with 1 twist	2	0	12	0	0	0	28	0	41	0	0
40	double salto backward piked	2	0	12	0	0	0	28	0	0	0	0
41	sissonne (leg separation 180 degree on the diagonal to the floor, take off two feet, land on one foot)	3	0	0	0	0	22	0	0	0	0	0
42	split jump with 0.5 turn in side position	3	0	0	0	0	19	0	32	0	0	0
43	split jump	3	0	0	0	0	19	0	0	0	0	0
44	straddle pike jump or side split jump	3	0	0	0	0	20	0	0	0	0	0
45	split ring jump (ring jump with front leg horizontal to the floor)	3	0	0	0	0	23	0	0	0	0	0
46	switch leap with 0.5 turn	3	0	0	0	0	16	0	32	0	0	0
47	switch leap (leap forward with leg change)	3	0	0	0	0	16	0	0	0	0	0
48	split leap forward	3	0	0	0	0	26	0	0	0	0	0
49	johnson (leap forward with leg change and 0.25 turn to side split or straddle pike position)	3	0	0	0	0	18	0	0	0	0	0
50	switch leap to ring position	3	0	0	0	0	16	30	0	0	0	0
51	sheep jump (jump with upper back arch and head release with feet to head height/closed Ring)	3	0	0	0	0	24	0	0	0	0	0
52	wolf hop or jump (hip angle at 45, knees together)	3	0	0	0	0	25	0	0	0	0	0
53	1 turn with heel of free leg forward at horizontal throughout turn	3	0	0	0	0	0	0	33	0	0	61
54	2 turn on one leg, free leg optional below horizontal	3	0	0	0	0	0	0	35	0	0	60
55	1 turn on one leg, free leg optional below horizontal	3	0	0	0	0	0	0	33	0	0	60
56	2 turn in tuck stand on one leg, free leg optional	3	0	0	0	0	0	29	35	0	0	60
57	salto backward tucked with 1 twist	3	0	7	0	0	0	29	0	41	0	0
58	salto backward tucked	3	0	7	0	0	0	29	0	0	0	0
59	salto backward stretched-step out (feet land successively)	3	0	7	0	0	0	27	0	0	0	63
60	salto backward stretched with legs together	3	0	7	0	0	0	27	0	0	0	58
61	salto sideward tucked, take off from one leg to side stand	3	0	8	0	0	0	29	0	0	0	64
62	free aerial cartwheel landing in cross position	3	0	0	0	14	0	0	0	0	0	0
63	salto forward tucked to cross stand	3	0	6	0	0	0	29	0	0	0	0
64	free aerial walkover forward, landing on one or both feet	3	0	0	0	15	0	0	0	0	0	62
65	jump backward, flic-flac take-off with 0.5 twist through handstand to walkover forward, also with support on one arm	3	0	0	13	15	0	0	0	40	0	65

Table 18: **Mapping of classes to their queries and responses in Gym99.** We show all the 99 classes in Gym99 and their responses to the 11 queries.

class id	class name	attribute id for each query										
		event	onto	tumbling	flic-flac	acrobatics	jump	position	turn	twist	circle	stand
66	flic-flac to land on both feet	3	0	0	13	0	0	0	0	0	0	62
67	flic-flac with step-out, also with support on one arm	3	0	0	13	0	0	0	0	0	0	63
68	round-off	3	5	0	0	0	0	0	0	0	0	0
69	double salto backward tucked	3	0	12	0	0	0	29	0	0	0	0
70	salto backward tucked	3	0	7	0	0	0	29	0	0	0	0
71	double salto backward piked	3	0	12	0	0	0	28	0	0	0	0
72	salto backward stretched with 2 twist	3	0	7	0	0	0	27	0	42	0	0
73	salto backward stretched with 2.5 twist	3	0	7	0	0	0	27	0	45	0	0
74	pike sole circle backward with 1 turn to handstand	4	0	0	0	0	0	28	33	0	47	65
75	pike sole circle backward with 0.5 turn to handstand	4	0	0	0	0	0	28	32	0	47	65
76	pike sole circle backward to handstand	4	0	0	0	0	0	28	0	0	47	65
77	giant circle backward with 1 turn to handstand	4	0	0	0	0	0	0	33	0	48	65
78	giant circle backward with 0.5 turn to handstand	4	0	0	0	0	0	0	32	0	48	65
79	giant circle backward	4	0	0	0	0	0	0	0	0	48	0
80	giant circle forward with 1 turn on one arm before handstand phase	4	0	0	0	0	0	0	33	0	49	65
81	giant circle forward with 0.5 turn to handstand	4	0	0	0	0	0	0	32	0	49	65
82	giant circle forward	4	0	0	0	0	0	0	0	0	49	0
83	clear hip circle backward to handstand	4	0	0	0	0	0	0	0	0	51	65
84	clear pike circle backward with 1 turn to handstand	4	0	0	0	0	0	28	33	0	50	65
85	clear pike circle backward with 0.5 turn to handstand	4	0	0	0	0	0	28	32	0	50	65
86	clear pike circle backward to handstand	4	0	0	0	0	0	28	0	0	50	65
87	stalder backward with 1 turn to handstand	4	0	0	0	0	0	0	33	0	46	65
88	stalder backward to handstand	4	0	0	0	0	0	0	0	0	46	65
89	counter straddle over high bar to hang	4	0	0	0	0	0	31	0	0	52	0
90	counter piked over high bar to hang	4	0	0	0	0	0	28	0	0	52	0
91	(swing backward or front support) salto forward straddled to hang on high bar	4	0	6	0	0	0	31	0	0	54	0
92	(swing backward) salto forward piked to hang on high bar	4	0	6	0	0	0	28	0	0	54	0
93	(swing forward or hip circle backward) salto backward with 0.5 turn piked to hang on high bar	4	0	7	0	0	0	28	32	0	51	0
94	transition flight from high bar to low bar	4	0	0	0	0	0	0	0	0	55	0
95	transition flight from low bar to high bar	4	0	0	0	0	0	0	0	0	56	0
96	(swing forward) double salto backward tucked with 1 turn	4	0	12	0	0	0	29	33	0	53	0
97	(swing backward) double salto forward tucked	4	0	11	0	0	0	29	0	0	54	0
98	(swing forward) double salto backward stretched	4	0	12	0	0	0	27	0	0	53	0